

---

# Linear Classifiers in Product Space Forms

---

**Puoya Tabaghi**

Coordinated Science Lab  
ECE Department, UIUC  
tabaghi2@illinois.edu

**Eli Chien**

Coordinated Science Lab  
ECE Department, UIUC  
ichien3@illinois.edu

**Chao Pan**

Coordinated Science Lab  
ECE Department, UIUC  
chaopan2@illinois.edu

**Jianhao Peng**

Coordinated Science Lab  
ECE Department, UIUC  
jianhao2@illinois.edu

**Olgica Milenkovic**

Coordinated Science Lab  
ECE Department, UIUC  
milenkov@illinois.edu

## Abstract

Embedding methods for product spaces are powerful techniques for low-distortion and low-dimensional representation of complex data structures. Nevertheless, little is known regarding downstream learning and optimization problems in such spaces. Here, we address the problem of linear classification in a product space form – a mix of Euclidean, spherical, and hyperbolic spaces. First, we describe new formulations for linear classifiers on a Riemannian manifold using geodesics and Riemannian metrics which generalize straight lines and inner products in vector spaces, respectively. Second, we prove that linear classifiers in  $d$ -dimensional space forms of any curvature have the same expressive power, i.e., they can shatter exactly  $d + 1$  points. Third, we formalize linear classifiers in product space forms, describe the first corresponding perceptron and SVM classification algorithms, and establish rigorous convergence results for the former. We support our theoretical findings with simulation results on several datasets, including synthetic data, CIFAR-100, MNIST, Omniglot, and single-cell RNA sequencing data. The results show that learning methods applied to small-dimensional embeddings in product space forms outperform their algorithmic counterparts in each space form.

## 1 Introduction

Euclidean spaces have been the focal point of machine learning studies since many practical datasets inherently lie in such spaces and are easy to represent and process using Euclidean geometry. Nevertheless, non-Euclidean spaces have recently been shown to provide significantly improved representations compared to Euclidean spaces for various data structures [1] and measurement modalities (e.g., metric and non-metric) [2, 3]. Examples include *hyperbolic spaces*, suitable for representing hierarchical data associated with graphs [4, 5] as well as human-interpretable images [6]; and *spherical spaces*, which are well-suited for capturing similarities in text embeddings and cycle-structures in graphs [7, 8]. Another important contribution in the area of non-Euclidean representation learning was described in [8], pertaining to learning methods for finding “good” mixed-curvature or hyperbolic representations for various types of complex heterogeneous datasets. All three spaces considered – hyperbolic, Euclidean, and spherical – have *constant curvatures* but differ in terms of their curvature signs (negative, zero and positive, respectively).

Despite these recent advances in nontraditional space data embeddings, almost all accompanying learning approaches for nonstandard space forms have focused on (heuristic) designs of neural network models for constant curvature spaces [9–15]. The fundamental building blocks of these neural networks, the perceptron, has received little attention outside the domain of learning in

Euclidean spaces. Exceptions include two studies of linear classifiers (perceptrons and SVMs) in purely hyperbolic spaces [16, 17]. Although discussed within a limited context in [18, 9], classification in product spaces remains largely unexplored, especially from the theoretical aspect.

Here, we address for the first time the problem of designing linear classifiers for product space forms (and generally, for geodesically complete Riemannian manifolds) with provable performance guarantees. Product space forms arise in a variety of applications in which graph-structured data captures both cycles and tree-like entities; examples of particular interest include social networks, such as the Facebook network for which product spaces reduce the embedding distortion by more than 30% when compared to Euclidean or hyperbolic spaces alone [8]. An important property of such spaces is that they are endowed with logarithmic and exponential maps which play a crucial role in establishing rigorous performance results. We first show that our classifiers for  $d$ -dimensional spaces can shatter  $d + 1$  points regardless of the curvature. We then describe the key ideas behind our analysis: Defining separation surfaces in constant curvature spaces directly through the use of geodesics on Riemannian manifolds (this definition matches the one proposed in [10, 14] for implementing hyperbolic neural networks); and, introducing metrics that render distances in different spaces compatible with each other and integrate them into one “majority” signed distance. One particular distance-based classifier, our product space form perceptron, is extremely simple to implement, flexible and it relies on a small (reduced) number of parameters. The new perceptron algorithm comes with provable performance guarantees established via the use of indefinite kernels and their Taylor series analysis. This proof technique significantly departs from classification methods in purely hyperbolic spaces [16, 17] and it allows for generalizations to SVMs, discussed in Section 4.2.

From the practical point of view, we demonstrate that our product space perceptron offers excellent performance on both synthetic product-space data and real-world datasets, such as the simple MNIST [19] and Omniglot [20] datasets, but also more complex structures such as CIFAR-100 [21] and single-cell expression measurements [22–24] which are indispensable in computational biology, when compared to similar methods in Euclidean, spherical, or hyperbolic spaces only which ignore the “hybrid” geometry of the data. The gains on the latter two sets are presented in Section 5.

The paper is organized as follows. In Sections 2 and 3 we review a special representation of linear classifiers in  $d$ -dimensional constant curvature spaces, e.g., Euclidean, hyperbolic and spherical spaces, and prove that distance-based classifiers have the same expressive power: Their Vapnik-Chervonenkis dimension equals  $d + 1$ . Section 4 contains our main results, a description of an approach for generalizing linear classifiers in space forms to product spaces, the first example of a product space form perceptron algorithm that performs provably optimal classification in a finite number of steps, and the first implementation of a product space form SVM algorithm. Section 5 and the Supplement contain our simulation results pertaining to synthetic data, MNIST, Omniglot, CIFAR-100 and single-cell expression data. All proofs are delegated to the Supplement.

## 2 Linear Classifiers in Euclidean Space

Finite-dimensional Euclidean spaces are inner product vector spaces over the reals. In contrast, hyperbolic and (hyper)spherical spaces do not have the structure of a vector space. Therefore, we first have to clarify what linear classification means in spaces with nonzero curvatures. To introduce our approach, we begin by recasting the definition of Euclidean linear classifiers in terms of commonly used concepts in differential geometry such as geodesics and Riemannian metrics [25]. This will allow us to (1) present a unified way of viewing the classification procedure in metric spaces that are not necessarily vector spaces; (2) formalize *distance-based* linear classifiers in space forms, i.e., classifiers that label data points based on their *signed distances* to the separation surface (Section 3); and (3) use the aforementioned classifiers as canonical building blocks for linear classifiers in product space forms (Section 4).

In a linear (more precisely, affine) binary classification problem we are given a set of  $N$  points in a Euclidean space and their binary labels, i.e.,  $(x_n, y_n) \in \mathbb{R}^d \times \{-1, 1\}$  for  $n \in [N] \stackrel{\text{def}}{=} \{1, \dots, N\}$ . The goal is to learn a linear classifier that produces the most accurate estimate of the labels. We define a linear classifier with weight  $w \in \mathbb{R}^d$  and bias  $b \in \mathbb{R}$  as

$$l_{b,w}^{\mathbb{E}}(x) = \text{sgn}(w^\top x + b), \quad (1)$$

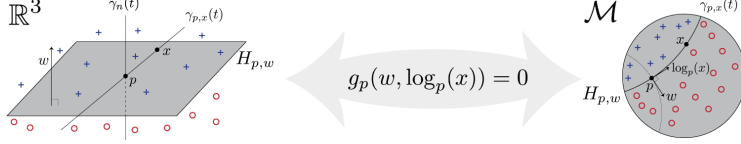


Figure 1: Linear classifiers in a 3-dimensional Euclidean space (left) and on a manifold (right).

where  $\|w\|_2 = 1$ , and  $l_{b,w}^{\mathbb{E}}(x)$  denotes the estimated label of  $x \in \mathbb{R}^d$  for the given classifier parameters  $b, w$ . The expression (1) may be reformulated in terms of a “point-line” pair as follows: Let  $p$  be any point on the decision boundary and  $w$  a corresponding normal vector. Then, we have

$$l_{b,w}^{\mathbb{E}}(x) = \text{sgn}(\langle w, x - p \rangle), \quad (2)$$

where  $b = -p^\top w$  and  $\langle \cdot, \cdot \rangle$  stands for the dot product. Simply put, the linear classifier returns the sign of the inner product of tangent vectors of two straight lines, namely

$$\gamma_{p,x}(t) = (1-t)p + tx \quad \text{and} \quad \gamma_n(t) = p + tw, \quad (3)$$

at their point of intersection  $p \in \mathbb{R}^d$  (see Figure 1). Here,  $\gamma_n$  is the normal line and  $\gamma_{p,x}$  is the line determined by  $p$  and the point  $x$  whose label we want to determine. Note that these lines are smooth curves parameterized by  $t \in [0, 1]$  (or an open interval in  $\mathbb{R}$ ), which we interpret as *time*.

The linear classifier in (2) can be reformulated as  $l_{b,w}^{\mathbb{E}}(x) = \text{sgn}(\langle \frac{d}{dt} \gamma_{p,x}(t)|_{t=0}, \frac{d}{dt} \gamma_n(t)|_{t=0} \rangle)$ , where the derivative of a line  $\gamma(t)$  at time 0 represents the *tangent vector* (or *velocity*) at the point  $p = \gamma(0)$ . This particular formulation leads to the following intuitive definition of linear classifiers in Euclidean spaces, which can be individually generalized for hyperbolic and spherical spaces.

**Definition 1.** *A linear classifier in Euclidean space returns the sign of the inner product between tangent vectors of two straight lines described in (3) that meet at a unique point.*

Often, we are interested in large-margin Euclidean linear classifiers for which we have  $y_n \langle w, x_n - p \rangle \geq \varepsilon$ , for all  $n \in [N]$ , and some margin  $\varepsilon > 0$ . For distance-based classifiers, we want  $\varepsilon$  to relate to the distance between the points  $x_n$  and the separation surface. For the classifier in (2), the distance between a point  $x \in \mathbb{R}^d$  and the classification boundary, defined as  $H_{p,w} = \{x \in \mathbb{R}^d : \langle w, x - p \rangle = 0\}$ , can be computed as

$$\min_{y \in H_{p,w}} d(x, y) = |\langle w, x - p \rangle| = |w^\top x + b|.$$

Note that in the point-line definition (2), the point  $p$  can be anywhere on the decision boundary and it has  $d$  degrees of freedom whereas  $b$  from definition (1) is a scalar parameter. Therefore, we prefer definition (1) as it represents a distance-based Euclidean classifier with only  $d + 1$  free parameters –  $w$  and  $b$  – and a norm constraint,  $\langle w, w \rangle = 1$ . In Section 3, we show that distance-based classifiers in  $d$ -dimensional space forms – of any curvature – can be defined with  $d + 1$  free parameters and a norm constraint.

### 3 Linear Classifiers in Space Forms

A space form is a complete, simply connected Riemannian manifold of dimension  $d \geq 2$  and constant curvature. Space forms are equivalent to spherical, Euclidean, or hyperbolic spaces up to an isomorphism [26]. To define linear classifiers in space forms, we first review fundamental concepts from differential geometry such as geodesics, tangent vectors and Riemannian metrics needed to generalize the key terms in Definition 1. For a detailed review, see [27, 25].

Let  $\mathcal{M}$  be a Riemannian manifold and let  $p \in \mathcal{M}$ . The tangent space at the point  $p$ , denoted by  $T_p \mathcal{M}$ , is the collection of all tangent vectors at  $p$ . The Riemannian metric  $g_p : T_p \mathcal{M} \times T_p \mathcal{M} \rightarrow \mathbb{R}$  is given by a positive-definite inner product in the tangent space  $T_p \mathcal{M}$  which depends smoothly on the base point  $p$ . A Riemannian metric generalizes the notion of inner products for Riemannian manifolds. The norm of a tangent vector  $v \in T_p \mathcal{M}$  is given by  $\|v\| = \sqrt{g_p(v, v)}$ . The length of a smooth curve

$\gamma : [0, 1] \rightarrow \mathcal{M}$  (or path) can be computed as  $L[\gamma] = \int_0^1 \|\gamma'(t)\| dt$ . A geodesic  $\gamma_{p_1, p_2}$  on a manifold is the shortest-length smooth path between the points  $p_1, p_2 \in \mathcal{M}$ ,

$$\gamma_{p_1, p_2} = \arg \min_{\gamma} L[\gamma] : \gamma(0) = p_1, \gamma(1) = p_2;$$

a geodesic generalizes the notion of a straight line in Euclidean space. Next, consider a geodesic  $\gamma(t)$  starting at  $p$  and with initial velocity  $v \in T_p \mathcal{M}$ , e.g.,  $\gamma(0) = p$  and  $\gamma'(0) = v$ . The exponential map gives the position of this geodesic at  $t = 1$ , i.e.,  $\exp_p(v) = \gamma(1)$ . Conversely, the logarithmic map is its inverse, i.e.,  $\log_p = \exp_p^{-1} : \mathcal{M} \rightarrow T_p \mathcal{M}$ . In other words, for two points  $p$  and  $x \in \mathcal{M}$ , the logarithmic map  $\log_p(x)$  gives the initial velocity (tangent vector) at which we can move – along the geodesic – from  $p$  to  $x$  in one time step. In geodesically complete Riemannian manifolds, the exponential and logarithmic maps are well-defined operators. Therefore, analogous to Definition 1, we can define a general notion of linear classifiers as described next.

**Definition 2.** Let  $(\mathcal{M}, g)$  be a geodesically complete Riemannian manifold, let  $p \in \mathcal{M}$  and let  $w \in T_p \mathcal{M}$  be a normal vector. A linear classifier  $l_{p, w}$  over the manifold  $\mathcal{M}$  is defined as

$$l_{p, w}^{\mathcal{M}}(x) = \text{sgn}(g_p(w, \log_p(x))), \text{ where } x \in \mathcal{M}.$$

Despite its generality, Definition 2 has the following drawbacks: (1) It does not formalize a distance-based classifier since  $|g_p(w, \log_p(x))|$  is not necessarily related to the distance of  $x$  to the decision boundary; (2) For a fixed  $x \in \mathcal{M}$ , the decision rule  $g_p(w, \log_p(x))$  varies with the choice of  $p$ , which is an arbitrary point on the decision boundary; (3) Often, we can represent the decision boundary with other parameters that have a smaller number of degrees of freedom compared to that of  $w$  and  $p$  required by Definition 2 (see the Euclidean linear classifiers defined in (2) and (1)). We therefore next resolve these issues for linear classifiers in space forms.

### 3.1 Spherical Spaces

Let  $p \in \mathbb{S}^d$  and  $w \in T_p \mathbb{S}^d$  (see Table 1). The decision boundary is given by

$$H_{p, w} = \left\{ x \in \mathbb{S}^d : \langle w, \frac{\theta}{\sin(\theta)}(x - p \cos \theta) \rangle = 0 \right\} \stackrel{(a)}{=} \{x \in \mathbb{S}^d : w^\top x = 0\} = \mathbb{S}^d \cap w^\perp, \quad (4)$$

where (a) is due to the fact that  $w \in T_p \mathbb{S}^d = p^\perp$ . This formulation uses two parameters  $p \in \mathbb{S}^d$  and  $w \in T_p \mathbb{S}^d$  to define the decision boundary (4). We note that one can actually characterize the *same* boundary with fewer parameters. Observe that for any  $w \in \mathbb{R}^{d+1}$ , we can pick an arbitrary base vector  $p \in w^\perp \cap \mathbb{S}^d$  which ensures that  $w \in T_p \mathbb{S}^d$ . Therefore, without loss of generality, we can define the decision boundary using only one vector  $w \in \mathbb{R}^{d+1}$ , which has  $d + 1$  degrees of freedom. In Proposition 1, we identify a specific choice of  $p \in w^\perp \cap \mathbb{S}^d$  that allows us to classify each data point based on its signed distance from the classification boundary.

Table 1: Key properties of Euclidean ( $\mathbb{R}^d$ ), spherical ( $\mathbb{S}^d$ ), and hyperbolic (Loid,  $\mathbb{L}^d$ ) manifolds.

$\mathcal{M}$	$T_p \mathcal{M}$	$g_p(u, v)$	$\log_p(x) : \theta = d(x, p)$	$\exp_p(v)$	$d(x, p)$	$\gamma_{p, x}(t)$
$\mathbb{R}^d$	$\mathbb{R}^d$	$\langle u, v \rangle$	$x - p$	$p + v$	$\ x - p\ _2$	$(1 - t)p + tx$
$\mathbb{S}^d$	$p^\perp$	$\langle u, v \rangle$	$\frac{\theta}{\sin(\theta)}(x - p \cos \theta)$	$\cos \ v\  p + \sin(\ v\ ) \frac{v}{\ v\ }$	$\text{acos}(\langle x, p \rangle)$	$\frac{\sin(\theta(1-t))}{\sin \theta} p + \frac{\sin(\theta t)}{\sin \theta} x$
$\mathbb{L}^d$	$p^\perp$	$\langle u, v \rangle$	$\frac{\theta}{\sinh(\theta)}(x - p \cosh \theta)$	$\cosh \ v\  p + \sinh(\ v\ ) \frac{v}{\ v\ }$	$\text{acosh}(-\langle x, p \rangle)$	$\frac{\sinh(\theta(1-t))}{\sinh \theta} p + \frac{\sinh(\theta t)}{\sinh \theta} x$

**Proposition 1.** Let  $p \in \mathbb{S}^d$ ,  $w \in T_p \mathbb{S}^d$ , and  $H_{p,w}$  be the decision boundary in (4). If  $\langle w, w \rangle = 1$ , then

$$\forall x \in \mathbb{S}^d : \min_{y \in H_{p,w}} d(x, y) = \text{asin}|w^\top x| = |g_{p_\circ}^{\mathbb{S}}(w, \log_{p_\circ}(x))|,$$

where  $g^{\mathbb{S}}$  is the Riemannian metric for a spherical space given in Table 1, and  $p_\circ = \|P_w^\perp x\|^{-1} P_w^\perp x \in H_{p,w}$ . Here, the projection operator is defined as  $P_w^\perp x = x - \langle x, w \rangle w$ .

It is important to point out that the classification boundary is invariant with respect to the choice of the base vectors, i.e.,  $H_{p,w} = H_{p_\circ,w}$ . From Proposition 1, if we have

$$\forall n \in [N] : y_n \text{asin}(w^\top x_n) \geq \varepsilon,$$

then all data points are correctly classified and have the minimum distance of  $\varepsilon$  to the classification boundary. In summary, we can define distance-based linear classifiers in a spherical space as follows.

**Definition 3.** Let  $w \in \mathbb{R}^{d+1}$  with  $\langle w, w \rangle = 1$ . A spherical linear classifier is defined as

$$l_w^{\mathbb{S}}(x) = \text{sgn}(\text{asin}(\langle w, x \rangle)).$$

### 3.2 Hyperbolic Spaces

The Poincaré model of a  $d$ -dimensional hyperbolic space [28] is a Riemannian manifold  $\mathcal{L}^d = (\mathbb{L}^d, g^{\mathbb{H}})$  for which  $\mathbb{L}^d = \{x \in \mathbb{R}^{d+1} : [x, x] = -1, x_1 > 0\}$ , and  $g_p^{\mathbb{H}}(u, v)$  corresponds to the Lorentzian inner product of  $u$  and  $v \in T_p \mathbb{L}^d$ , defined as

$$[u, v] = u^\top H v, \quad H = \begin{pmatrix} -1 & 0^\top \\ 0 & I_d \end{pmatrix}, \quad (5)$$

where  $I_d$  is the  $d \times d$  identity matrix. Let  $p \in \mathbb{L}^d$  and  $w \in T_p \mathbb{L}^d$ . The classification boundary of interest is given by

$$H_{p,w} = \left\{ x \in \mathbb{L}^d : \left[ w, \frac{\theta}{\sinh(\theta)}(x - p \cos \theta) \right] = 0 \right\} = \{x \in \mathbb{L}^d : [w, x] = 0\} = \mathbb{L}^d \cap w^\perp. \quad (6)$$

Similar to the case of spherical spaces, we can simplify the formulation as follows. If  $w$  is a time-like vector – a vector that satisfies  $w \in \{x : [x, x] > 0\}$  [25] – and  $p \in \mathbb{L}^d \cap w^\perp$ , then we have  $w \in T_p \mathbb{L}^d$ . In Proposition 2, we derive the expression for a special  $p \in \mathbb{L}^d \cap w^\perp$  that allows us to formulate a distance-based hyperbolic linear classifier.

**Proposition 2.** Let  $p \in \mathbb{L}^d$ ,  $w \in T_p \mathbb{L}^d$ , and let  $H_{p,w}$  be the decision boundary in (6). If  $[w, w] = 1$ , then

$$\min_{y \in H_{p,w}} d(x, y) = \text{asinh}|[w, x]| = |g_{p_\circ}^{\mathbb{H}}(w, \log_{p_\circ}(x))|,$$

where  $g^{\mathbb{H}}$  is the Riemannian metric for the hyperbolic space (given in Table 1), and  $p_\circ = \|P_w^\perp x\|^{-1} P_w^\perp x \in H_{p,w}$ . Note that  $P_w^\perp x$  is the orthogonal projection of  $x$  onto  $w^\perp$ , i.e.,  $P_w^\perp x = x - [x, w]w$ . Therefore,  $p_\circ = \sqrt{\frac{1}{1+[x,w]^2}}(x - [x, w]w)$ .

As a result, we have the following definition of distance-based linear classifiers in a hyperbolic spaces.

**Definition 4.** Let  $w \in \mathbb{R}^{d+1}$  with  $[w, w] = 1$ . A hyperbolic linear classifier is defined as

$$l_w^{\mathbb{H}}(x) = \text{sgn}(\text{asinh}([w, x])).$$

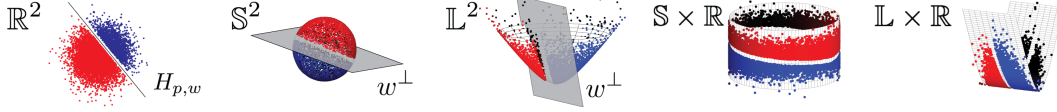


Figure 2: Linear classifiers in Euclidean, spherical, hyperbolic spaces and product spaces. A hyperbolic space has dimension  $\geq 2$ , but we reduced it to 1 for visualization purposes only.

From the previous discussion, we can deduce that *linear classifiers in  $d$ -dimensional space forms can be characterized with  $d + 1$  free parameters and a norm constraint*. This supports the following result pertaining to the Vapnik-Chervonenkis dimension [29] of linear classifiers in space forms.

**Theorem 1.** *The VC dimension of a linear classifier in a  $d$ -dimensional space form is  $d + 1$ .*

Figure 2 illustrates linear classifiers in 2-dimensional hyperbolic, Euclidean, spherical spaces and two product space forms. Next, we show how the first three classifiers – all of which have the same expressive power – can be “mixed” to define a linear classifier in product space forms.

## 4 Linear Classifiers in Product Space Forms

Definition 2 of linear classifiers applies to geodesically complete Riemannian manifolds but our focus will be on linear classifiers in product space forms. We now describe the first perceptron algorithm for such spaces that *provably* learns an optimal classifier for linearly separable points in a finite number of iterations. Then, we extend this learning scheme to large-margin classifiers in product space forms.

Consider a collection of Euclidean, spherical, and hyperbolic manifolds, e.g.,  $(\mathbb{E}^{d_{\mathbb{E}}}, g^{\mathbb{E}})$ ,  $(\mathbb{S}^{d_{\mathbb{S}}}, g^{\mathbb{S}})$ ,  $(\mathbb{H}^{d_{\mathbb{H}}}, g^{\mathbb{H}})$  with sectional curvatures 0,  $C_{\mathbb{S}}, C_{\mathbb{H}}$ , respectively (see the Supplement for detailed information on space forms with arbitrary curvatures). The Euclidean manifold is simply  $\mathbb{R}^{d_{\mathbb{E}}}$  while the hyperbolic space is the ‘Loid model  $\mathbb{L}^{d_{\mathbb{H}}}$ . The product manifold  $\mathcal{M} = \mathbb{E}^{d_{\mathbb{E}}} \times \mathbb{S}^{d_{\mathbb{S}}} \times \mathbb{H}^{d_{\mathbb{H}}}$  admits a canonical Riemannian metric  $g$ , called the *product Riemannian metric*. The tangent space of  $\mathcal{M}$  at a point  $p = (p_{\mathbb{E}}, p_{\mathbb{S}}, p_{\mathbb{H}})$  can be decomposed as [30]

$$T_p \mathcal{M} = \bigoplus_{S \in \{\mathbb{E}, \mathbb{S}, \mathbb{H}\}} T_{p_S} S^{d_S}, \quad (7)$$

where the right-hand side expression is the direct sum  $\bigoplus$  of individual tangent spaces  $T_{p_{\mathbb{E}}} \mathbb{E}^{d_{\mathbb{E}}}$ ,  $T_{p_{\mathbb{S}}} \mathbb{S}^{d_{\mathbb{S}}}$ , and  $T_{p_{\mathbb{H}}} \mathbb{H}^{d_{\mathbb{H}}}$ . The *scaled* Riemannian metric used on  $\mathcal{M}$  is

$$g_p(u, v) = \sum_{S \in \{\mathbb{E}, \mathbb{S}, \mathbb{H}\}} \alpha_S g_{p_S}^S(u_S, v_S), \quad (8)$$

where  $u = (u_{\mathbb{E}}, u_{\mathbb{S}}, u_{\mathbb{H}}), v = (v_{\mathbb{E}}, v_{\mathbb{S}}, v_{\mathbb{H}}) \in T_p \mathcal{M}$ ,  $p = (p_{\mathbb{E}}, p_{\mathbb{S}}, p_{\mathbb{H}})$ , and  $\alpha_{\mathbb{E}}, \alpha_{\mathbb{S}}, \alpha_{\mathbb{H}}$  are positive weights. The choice of the scaled Riemannian metric in Equation (8) – and hence the classification criteria – resolves the potential “distance compatibility” issues that arise from possibly vastly different ranges and variances of each component (e.g.,  $x_{\mathbb{E}}, x_{\mathbb{S}}$ , and  $x_{\mathbb{H}}$ ) which could lead to a classification criterion that is dominated by the component with the largest variance.

Based on our previous discussions, in order to describe linear classifiers on the above manifold  $\mathcal{M}$ , we first need to identify the logarithmic map (see Definition 2). For this purpose, we invoke the following known result that formalizes geodesics, exponential and logarithmic maps on  $\mathcal{M}$ .

**Fact 1.** [27] *Let  $\mathcal{M} = \mathbb{E}^{d_{\mathbb{E}}} \times \mathbb{S}^{d_{\mathbb{S}}} \times \mathbb{H}^{d_{\mathbb{H}}}$  with Riemannian metric given by (8). Then, the geodesics, exponential, and logarithmic maps on  $\mathcal{M}$  are the concatenation of the corresponding maps of the individual space forms, i.e.,  $\gamma(t) = (\gamma_{\mathbb{E}}(t), \gamma_{\mathbb{S}}(t), \gamma_{\mathbb{H}}(t))$ ,  $\exp_p(v) = (\exp_{p_{\mathbb{E}}}(v_{\mathbb{E}}), \exp_{p_{\mathbb{S}}}(v_{\mathbb{S}}), \exp_{p_{\mathbb{H}}}(v_{\mathbb{H}}))$ , and  $\log_p(x) = (\log_{p_{\mathbb{E}}}(x_{\mathbb{E}}), \log_{p_{\mathbb{S}}}(x_{\mathbb{S}}), \log_{p_{\mathbb{H}}}(x_{\mathbb{H}}))$ , where  $p = (p_{\mathbb{E}}, p_{\mathbb{S}}, p_{\mathbb{H}})$ ,  $x = (x_{\mathbb{E}}, x_{\mathbb{S}}, x_{\mathbb{H}}) \in \mathcal{M}$ ,  $v = (v_{\mathbb{E}}, v_{\mathbb{S}}, v_{\mathbb{H}}) \in T_p \mathcal{M}$ , and  $\gamma_{\mathbb{E}}, \gamma_{\mathbb{S}}, \gamma_{\mathbb{H}}$  are geodesics in their corresponding space form<sup>1</sup>.*

<sup>1</sup>The distance between  $x, y \in \mathcal{M}$  is given by  $d(x, y) = (\sum_{S \in \{\mathbb{E}, \mathbb{S}, \mathbb{H}\}} \alpha_S^2 d_S(x_S, y_S)^2)^{\frac{1}{2}}$ ; see Table 1.

Combining the results regarding distance-based linear classifiers in space forms (Section 3), the definition of tangent product spaces in terms of the product of tangent spaces in (7), and the choice of the Riemannian metrics given in Table 1, we arrive at the following formulation for a product space linear classifier. For detailed derivations, the reader is referred to the Supplement.

**Proposition 3.** *Let  $\mathbb{S}^{d_{\mathbb{S}}}$  and  $\mathbb{H}^{d_{\mathbb{H}}}$  be space forms with curvatures  $C_{\mathbb{S}} > 0$ , and  $C_{\mathbb{H}} < 0$ . Let  $\mathcal{M} = \mathbb{E}^{d_{\mathbb{E}}} \times \mathbb{S}^{d_{\mathbb{S}}} \times \mathbb{H}^{d_{\mathbb{H}}}$  with the metric given by (8). The linear classifier on  $\mathcal{M}$  is defined as*

$$l_w^{\mathcal{M}}(x) = \text{sgn}(\langle w_{\mathbb{E}}, x_{\mathbb{E}} \rangle + b + \alpha_{\mathbb{S}} \text{asin}(\langle w_{\mathbb{S}}, x_{\mathbb{S}} \rangle) + \alpha_{\mathbb{H}} \text{asinh}([w_{\mathbb{H}}, x_{\mathbb{H}}])),$$

where  $w_{\mathbb{E}}$ ,  $w_{\mathbb{S}}$  and  $w_{\mathbb{H}}$  have norms of  $\alpha_{\mathbb{E}}$ ,  $\sqrt{C_{\mathbb{S}}}$ , and  $\sqrt{-C_{\mathbb{H}}}$ , respectively.

This classifier can be associated with three linear classifiers, Euclidean, hyperbolic, and spherical space classifiers. For a point  $x = (x_{\mathbb{E}}, x_{\mathbb{S}}, x_{\mathbb{H}}) \in \mathcal{M}$ , the product space classifier takes a weighted vote based on the signed distances of each component (e.g,  $x_{\mathbb{E}}$ ,  $x_{\mathbb{S}}$ , and  $x_{\mathbb{H}}$ ) to its corresponding classifier’s boundary. Figure 2 illustrates two classifiers in product space forms.

#### 4.1 A Product Space Form Perceptron

We now turn our attention to an algorithmic method for training linear classifiers in Proposition 3. To establish provable performance guarantees, we assume that the datasets satisfy the  $\varepsilon > 0$  margin property, i.e.,

$$\forall (x, y) \in \mathcal{X} : y(w_{\mathbb{E}}^{\top} x_{\mathbb{E}} + b + \alpha_{\mathbb{S}} \text{asin}(w_{\mathbb{S}}^{\top} x_{\mathbb{S}}) + \alpha_{\mathbb{H}} \text{asinh}([w_{\mathbb{H}}, x_{\mathbb{H}}])) \geq \varepsilon, \quad (9)$$

where  $\mathcal{X}$  is the set of labeled training data,  $\|w_{\mathbb{E}}\|_2 = \alpha_{\mathbb{E}}$ ,  $\|w_{\mathbb{S}}\|_2 = \sqrt{C_{\mathbb{S}}}$ , and  $\sqrt{[w_{\mathbb{H}}, w_{\mathbb{H}}]} = \sqrt{-C_{\mathbb{H}}}$ .

The classification function is nonlinear in  $w_{\mathbb{S}}$  and  $w_{\mathbb{H}}$  and it requires equality constraints for all the weights involved. To **analyze** the classifier and allow for sequential updates of its parameters, we relax the norm constraints and propose perceptron updates in a Reproducing Kernel Hilbert Space (RKHS) which we denote by  $\mathcal{H}$ <sup>2</sup>. We seek a map  $\phi : \mathcal{M} \rightarrow \mathcal{H}$  to represent the classifier in (9) as an inner product of two vectors in  $\mathcal{H}$ , i.e.,  $l_w^{\mathcal{M}}(x) = \text{sgn}(\langle \psi(w), \phi(x) \rangle_{\mathcal{H}})$ , where  $\langle \cdot, \cdot \rangle_{\mathcal{H}}$  is the inner product defined on  $\mathcal{H}$ . The kernels  $K_{\mathbb{E}}(w_{\mathbb{E}}, x_{\mathbb{E}}) = w_{\mathbb{E}}^{\top} x_{\mathbb{E}} + b$  and  $K_{\mathbb{S}}(w_{\mathbb{S}}, x_{\mathbb{S}}) = \text{asin}(w_{\mathbb{S}}^{\top} x_{\mathbb{S}})$  are symmetric and positive definite. Hence, they lend themselves to the construction of a valid RKHS. Unfortunately,  $K_{\mathbb{H}}(w_{\mathbb{H}}, x_{\mathbb{H}}) = \text{asinh}([w_{\mathbb{H}}, x_{\mathbb{H}}])$  is an indefinite kernel. To resolve this issue, we introduce an indefinite operator  $M : \mathcal{H}' \rightarrow \mathcal{H}'$ , where  $\mathcal{H}' \supseteq \mathcal{H}$  is the set of functions  $\mathcal{M} \rightarrow \mathbb{R}$  and  $M^{\top} M = \text{Id}$ , with  $\text{Id}$  denoting the identity operator<sup>3</sup>. Therefore, we can write the classifier (9) as

$$l_w^{\mathcal{M}}(x) = \text{sgn}(\langle \psi(w), M\phi(x) \rangle_{\mathcal{H}}), \quad (10)$$

where  $\psi(w), \phi(x) \in \mathcal{H}'$ , and  $\langle \cdot, M\cdot \rangle_{\mathcal{H}}$  is also well-defined on  $\mathcal{H}'$ . This separable form allows us to formulate the update rule of the perceptron in  $\mathcal{H}'$ . Note that the decision rule (10) only depends on the inner products of vectors in  $\mathcal{H}'$ , i.e., kernel function evaluations for a point  $x$  and the misclassified training data points (see Algorithm 1). In Theorem 2, we prove that the product space perceptron in Algorithm 1 converges in a finite number of steps.

---

#### Algorithm 1 A Product Space Form Perceptron

---

**Input:**  $\{x_n, y_n\}_{n=1}^N$ : a set of pairs of point-labels in  $\mathcal{M} \times \{-1, 1\}$ ;

**Initialization:**  $k = 0, n = 1, x \stackrel{\text{def}}{=} (x_{\mathbb{E}}, x_{\mathbb{S}}, x_{\mathbb{H}})$ ;

**repeat**

**if**  $\text{sgn}(l_k(x_n)) \neq y_n$  **then**

$$l_{k+1}(x) = l_k(x) + y_n (x_{\mathbb{E},n}^{\top} x_{\mathbb{E}} + 1 + \alpha_{\mathbb{S}} \text{asin}(C_{\mathbb{S}} x_{\mathbb{S},n}^{\top} x_{\mathbb{S}}) + \alpha_{\mathbb{H}} \text{asinh}(\frac{\langle x_{\mathbb{H},n}, x_{\mathbb{H}} \rangle}{R^2})) \rightarrow k = k + 1$$

**end if**

$n = \text{mod}(n, N) + 1$

**until** convergence criteria is met

---

<sup>2</sup>This kernel approach is used to establish convergence results and is not a part of the algorithmic solution.

<sup>3</sup>The operator  $M$  can be obtained by analyzing the Taylor series of  $\text{asinh}(\cdot)$ , as explained in the Supplement.



**Theorem 2.** Let  $\{x_n, y_n\}_{n=1}^N$  be points in a compact subset of  $\mathcal{M}$  with labels in  $\{-1, 1\}$ , and  $\|x_{\mathbb{H},n}\|_2 \leq R$  for all  $n \in [N]$ . If the point set is  $\varepsilon$ -margin linearly separable and  $\|w_{\mathbb{H}}\|_2 \leq 1/R$ , then Algorithm 1 converges in  $O(\frac{1}{\varepsilon^2})$  steps.

#### 4.1.1 Related Works and the Hyperbolic Perceptron

Linear classifiers in spherical spaces have been studied in a number of works [31, 32], while more recent work has focused on linear classifiers in the Poincaré model of hyperbolic spaces, in the context of hyperbolic neural networks [10]. A purely hyperbolic perceptron was described in [17]. Simulation evidence and some straightforward counterexamples show that the algorithm does not converge (see the Supplement for details). We therefore propose a modified update rule for a purely hyperbolic perceptron which is of independent interest given many emerging learning paradigms in hyperbolic spaces. Our hyperbolic perceptron uses a specialized update direction and provably converges, as described below (see more details in the Supplement).

**Theorem 3.** Let  $\{x_n, y_n\}_{n=1}^N$  be a labeled point set from a bounded subset of  $\mathbb{H}^{d_{\mathbb{H}}}$ . Assume the point set is linearly separable by a margin  $\varepsilon$ . Then, the hyperbolic perceptron with the update rule  $\text{sgn}([w^k, x_n]) \neq y_n : w^{k+1} = w^k + y_n H x_n$ , converges in  $O\left(\frac{1}{\sinh^2(\varepsilon)}\right)$  steps.

#### 4.2 A Product Space Form SVM

In the previous section, we showed that the classification criterion for linear classifiers defined in Proposition 3 is a linear function of the *feature* vectors, or, more precisely, of  $\{M\phi(x_n)\}_{n \in [N]}$ . This fact and the subsequent performance guarantees are due to the update rule operating in the RKHS which, in effect, lifts a finite dimensional point to a feature vector. Here, we use this analysis to formulate large-margin classifiers in product space forms. The idea behind our algorithm is to use the feature vector representation of linear classifiers, and maximize the distance between the points and the classification boundary. However, the exact closed-form of this distance is not available. But we can still provide an upper bound for this distance and perform maximum-margin classification. The described solution complements and extends the prior work on hyperbolic SVMs [16].

Let  $x_1, \dots, x_N \in \mathcal{M}$  be a fixed set of points. The *representer theorem* establishes the set of feasible parameters – in the space  $\mathcal{H}'$  – as a linear combinations of measured feature vectors. In other words, any estimated parameter  $\hat{w}_N$  must satisfy  $\psi(\hat{w}_N) \in \mathcal{L} = \{\sum_{n \in [N]} \beta_n M\phi(x_n) : \sum_{n \in [N]} \beta_n^2 < \infty\}$ . Let us assume that  $\psi(w) = \sum_{n \in [N]} \beta_n M\phi(x_n)$ . Then, the classification criterion is a linear function of  $\beta = (\beta_1, \dots, \beta_N)$ , i.e.,

$$l_w^{\mathcal{M}}(x) = \text{sgn}\left(\sum_{n \in [N]} \beta_n \langle \phi(x), \phi(x_n) \rangle_{\mathcal{H}}\right) = \text{sgn}\left(\sum_{n \in [N]} \beta_n k(x_n, x)\right) \quad (11)$$

where  $k(x, x_n) = 1 + x_{\mathbb{E}}^{\top} x_{\mathbb{E},n} + \alpha_{\mathbb{S}} \text{asin}(C_{\mathbb{S}} x_{\mathbb{S}}^{\top} x_{\mathbb{S},n}) + \alpha_{\mathbb{H}} \text{asin}(R^{-2} x_{\mathbb{H}}^{\top} x_{\mathbb{H},n})$ . In Algorithm 1, the weights are sequentially updated after each miss-classification. Here, we directly optimize the weight vector  $\beta$  to ensure the maximum separability condition. In Proposition 4, we derive necessary conditions for the vector  $\beta$  that are conducive to a proper distance-based classifier.

**Proposition 4.** For the classifier in (11), we have the following equivalent conditions:

- $\langle w_{\mathbb{E}}, w_{\mathbb{E}} \rangle = \alpha_{\mathbb{E}}^2 \Rightarrow \beta^{\top} K_{\mathbb{E}} \beta = \alpha_{\mathbb{E}}^2$ , where  $K_{\mathbb{E}} = (x_{\mathbb{E},i}^{\top} x_{\mathbb{E},j})_{i,j \in [N]}$
- $\langle w_{\mathbb{S}}, w_{\mathbb{S}} \rangle = C_{\mathbb{S}} \Rightarrow \beta^{\top} K_{\mathbb{S}} \beta = \frac{\pi}{2}$ , where  $K_{\mathbb{S}} = (\text{asin}(C_{\mathbb{S}} x_{\mathbb{S},i}^{\top} x_{\mathbb{S},j}))_{i,j \in [N]}$
- $[w_{\mathbb{H}}, w_{\mathbb{H}}] = -C_{\mathbb{H}} \Rightarrow \beta^{\top} K_{\mathbb{H}} \beta = \text{asinh}(-R^2 C_{\mathbb{H}})$ , where  $K_{\mathbb{H}} = (\text{asinh}(R^{-2} [x_{\mathbb{H},i}, x_{\mathbb{H},j}]))_{i,j \in [N]}$

The constraints in Proposition 4, if they are met, define a product space form classifier in which the classification margin is the sum ( $\ell_1$  norm) of the distances of the individual space components to the corresponding classifiers, which is related to the weighted vote majority classification approach



of Section 4. This distance is a proper upper bound (or a proxy) for the *true* distance of a point to the classification boundary which involves computing the  $\ell_2$  norm of the individual components' distances; see the footnote for Fact 1.

To convexify the constraint sets in Proposition 4, we replace the Euclidean and spherical constraints with their convex hulls. The hyperbolic constraint,  $[w_{\mathbb{H}}, w_{\mathbb{H}}] = -C_{\mathbb{H}}$ , leads to a nonconvex second-order equality constraint on  $\beta$ . We let  $K_{\mathbb{H}} = K_{\mathbb{H}}^+ - K_{\mathbb{H}}^-$  for two positive semidefinite matrices. Then, we relax this second order condition to  $\beta^\top K_{\mathbb{H}}^- \beta \leq r$  and  $\beta^\top K_{\mathbb{H}}^+ \beta \leq r + \text{asinh}(-R^2 C_{\mathbb{H}})$  for a small  $r > 0$ , i.e., we have  $-r < \beta^\top K_{\mathbb{H}} \beta < r + \text{asinh}(-R^2 C_{\mathbb{H}})$ . The Algorithm 2 is our proposed soft-margin SVM classifier, for points with noisy labels, in product space forms.

## 5 Numerical Experiments: Real-World Datasets

We illustrate the practical performance of our product space form classifiers – Algorithms 1 and 2 – on (1) CIFAR-100 [21] (100 classes of size 600 each) and two scRNA datasets (2) Lymphoma/Healthy donor with a targeted set of genes (2 classes with 13, 410 samples total), and (3) blood cells with 965 landmark genes [33] only (landmark genes can be used to infer the activities of all other genes, and in this case we had 10 classes with 94, 655 samples total) [22–24]. In the Supplement, we present the convergence of our classifiers on synthetic datasets, Omniglot and MNIST datasets which are not included in the main text due to space limitations.

We use the mixed-curvature VAEs algorithm [18] to embed each dataset into chosen (product) space forms. We perform binary classification for all class pairs, except for CIFAR-100 in which we only select 100 pairs. *Perceptron*: We split the data into 80% training and 20% test points. We allow all perceptron algorithms to go over the whole dataset only once. Then, we report the mean accuracy results with a confidence interval derived from repeated trials. *SVM*: A purely hyperbolic SVM is discussed in [16]. To train a product space form SVM, we relax the optimization problem by removing the hyperbolic constraints to improve the run time of the method; see Algorithm 2. For each dataset, we only use 100 training samples, and reserve the remaining samples for testing. We compute the mean accuracy and the confidence levels for all selected class pairs and repeated trials.

The results across different datasets, learning methods, and embedding signatures (i.e., choices of dimensions of the components in the product spaces) suggest that product spaces can offer better low-dimensional representations for complex data structures, especially for scRNA sequencing data; see Figure 3 and Table 5. Generally, a higher dimensional signature should lead to a better classification accuracy. However, the performance of the classification method is directly dependent on the quality of discriminative features extracted from the mixed-curvature VAEs. This algorithm is not guaranteed to improve the embedding quality with increased dimensions when hyperparameters are fixed. Furthermore, finding a signature that allows for near-optimal embedding distortion is a hard question that requires a sophisticated analysis of the geometry of datasets, and beyond the scope of this work. The improvements in classification accuracy for the CIFAR-100 data appear modest  $\sim 2\%$  but the performance of product space classifiers on the single-cell datasets is outstanding, with more than 30% improvements compared to individual space forms. This is not surprising given the prior biological insight that populations of cells in a tissue follow hierarchical evolutionary trajectories (suitably captured by hyperbolic spaces) and cyclic cell-cycle phases (suitably captured by spherical spaces). For a more detailed discussion, please refer to the Supplement.

---

### Algorithm 2 A Product Space Form SVM

---

**Input:**  $\{x_n, y_n\}_{n=1}^N$ : a set of point-labels in  $\mathcal{M} \times \{-1, 1\}$ . Let  $r > 0$ . Then, solve for  $\beta$  according to:

$$\text{maximize} \quad \epsilon - \sum_{n \in [N]} \zeta_n$$

$$\text{w.r.t} \quad \epsilon > 0, \{\zeta_n \geq 0\}$$

$$\text{subject to} \quad \forall n \in [N]: y_n \sum_{m \in [N]} \beta_m k(x_n, x_m) \geq \epsilon - \zeta_n$$

$$\beta \in \left\{ t: t^\top K_{\mathbb{E}} t < \alpha_{\mathbb{E}}^2, t^\top K_{\mathbb{S}} t < \frac{\pi}{2}, t^\top K_{\mathbb{H}}^- t \leq r, t^\top K_{\mathbb{H}}^+ t \leq r + \text{asinh}(-R^2 C_{\mathbb{H}}) \right\}$$


---

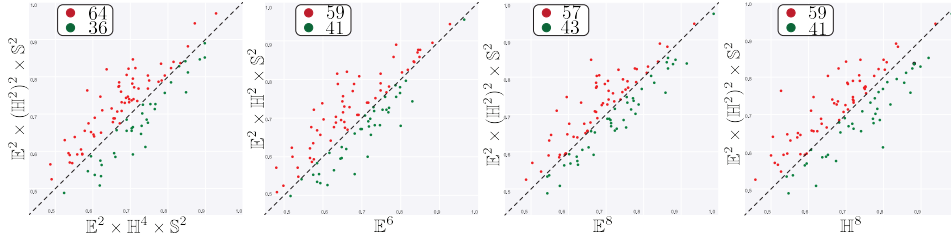


Figure 3: Classification accuracy of different product space form perceptrons on CIFAR-100 datasets. The labels on the  $x$  and  $y$  axis indicate the embedding spaces, and the counts in the top-left-corner indicate how often a binary classifier in one space outperforms that in another.

Table 2: Classification mean accuracy (%)  $\pm$  95% confidence interval for perceptron (P) and SVM (S) algorithms in a product space ( $d_E, d_H, d_S$ ). Datasets are CIFAR-100 (CFR), Lymphoma (LMPH), and Blood-cells-landmark (BCL).

$(d_E, d_H, d_S)$	(2, 2, 2)	(6, 0, 0)	(2, 2 <sup>2</sup> , 2)	(2, 4, 2)	(8, 0, 0)	(0, 8, 0)
(P)-CFR	70.26 $\pm$ 1.34	68.58 $\pm$ 1.29	<b>71.23 <math>\pm</math> 1.28</b>	69.93 $\pm$ 1.25	69.96 $\pm$ 1.29	69.90 $\pm$ 1.43
$(d_E, d_H, d_S)$	(2, 2, 2)	(6, 0, 0)	(0, 6, 0)	(0, 0, 6)	(2, 2 <sup>2</sup> , 2)	(8, 0, 0)
(P)-LMPH	<b>94.33 <math>\pm</math> 1.89</b>	59.16 $\pm$ 11.56	46.66 $\pm$ 9.1	44.69 $\pm$ 9.01	75.42 $\pm$ 11.97	59.16 $\pm$ 8.51
(P)-BCL	70.79 $\pm$ 6.26	66.03 $\pm$ 6.83	65.01 $\pm$ 3.84	62.41 $\pm$ 3.89	<b>72.33 <math>\pm</math> 5.79</b>	66.85 $\pm$ 6.30
(S)-LMPH	<b>94.48 <math>\pm</math> 1.31</b>	70.61 $\pm$ 1.59	50.68 $\pm$ 7.03	43.9 $\pm$ 0.004	91.44 $\pm$ 2.38	65.83 $\pm$ 3.42
(S)-BCL	83.17 $\pm$ 5.42	74.61 $\pm$ 5.39	57.62 $\pm$ 8.15	74.18 $\pm$ 5.19	<b>89.89 <math>\pm</math> 7.09</b>	77.75 $\pm$ 8.15

## References

- [1] Michael M Bronstein, Joan Bruna, Yann LeCun, Arthur Szlam, and Pierre Vandergheynst. Geometric deep learning: going beyond Euclidean data. *IEEE Signal Processing Magazine*, 34(4):18–42, 2017.
- [2] Puoya Tabaghi and Ivan Dokmanić. Hyperbolic distance matrices. In *Proceedings of the 26th ACM SIGKDD International Conference on Knowledge Discovery & Data Mining*, pages 1728–1738, 2020.
- [3] Puoya Tabaghi and Ivan Dokmanić. Geometry of comparisons. *arXiv preprint arXiv:2006.09858*, 2020.
- [4] Maximillian Nickel and Douwe Kiela. Poincaré embeddings for learning hierarchical representations. In *Advances in neural information processing systems*, pages 6338–6347, 2017.
- [5] Frederic Sala, Chris De Sa, Albert Gu, and Christopher Ré. Representation tradeoffs for hyperbolic embeddings. In *International conference on machine learning*, pages 4460–4469. PMLR, 2018.
- [6] Valentin Khruikov, Leyla Mirvakhabova, Evgeniya Ustinova, Ivan Oseledets, and Victor Lempit-sky. Hyperbolic image embeddings. In *Proceedings of the IEEE/CVF Conference on Computer Vision and Pattern Recognition*, pages 6418–6428, 2020.
- [7] Yu Meng, Jiaxin Huang, Guangyuan Wang, Chao Zhang, Honglei Zhuang, Lance Kaplan, and Jiawei Han. Spherical text embedding. In *Advances in Neural Information Processing Systems*, pages 8208–8217, 2019.
- [8] Albert Gu, Frederic Sala, Beliz Gunel, and Christopher Ré. Learning mixed-curvature representations in product spaces. In *International Conference on Learning Representations*, 2018.
- [9] Gregor Bachmann, Gary Bécigneul, and Octavian Ganea. Constant curvature graph convolutional networks. In *International Conference on Machine Learning*, pages 486–496. PMLR, 2020.

- [10] Octavian-Eugen Ganea, Gary Bécigneul, and Thomas Hofmann. Hyperbolic neural networks. *arXiv preprint arXiv:1805.09112*, 2018.
- [11] Ines Chami, Zhitao Ying, Christopher Ré, and Jure Leskovec. Hyperbolic graph convolutional neural networks. In *Advances in neural information processing systems*, pages 4868–4879, 2019.
- [12] Alexandru Tifrea, Gary Bécigneul, and Octavian-Eugen Ganea. Poincaré GloVe: Hyperbolic word embeddings. *arXiv preprint arXiv:1810.06546*, 2018.
- [13] Qi Liu, Maximilian Nickel, and Douwe Kiela. Hyperbolic graph neural networks. In *Advances in Neural Information Processing Systems*, pages 8230–8241, 2019.
- [14] Ryohei Shimizu, Yusuke Mukuta, and Tatsuya Harada. Hyperbolic neural networks++. *arXiv preprint arXiv:2006.08210*, 2020.
- [15] Jindou Dai, Yuwei Wu, Zhi Gao, and Yunde Jia. A hyperbolic-to-hyperbolic graph convolutional network. *arXiv preprint arXiv:2104.06942*, 2021.
- [16] Hyunghoon Cho, Benjamin DeMeo, Jian Peng, and Bonnie Berger. Large-margin classification in hyperbolic space. In *The 22nd International Conference on Artificial Intelligence and Statistics*, pages 1832–1840. PMLR, 2019.
- [17] Melanie Weber, Manzil Zaheer, Ankit Singh Rawat, Aditya Menon, and Sanjiv Kumar. Robust large-margin learning in hyperbolic space. *arXiv preprint arXiv:2004.05465*, 2020.
- [18] Ondrej Skopek, Octavian-Eugen Ganea, and Gary Bécigneul. Mixed-curvature variational autoencoders. In *International Conference on Learning Representations*, 2020.
- [19] Yann LeCun, Léon Bottou, Yoshua Bengio, and Patrick Haffner. Gradient-based learning applied to document recognition. *Proceedings of the IEEE*, 86(11):2278–2324, 1998.
- [20] Brenden M Lake, Ruslan Salakhutdinov, and Joshua B Tenenbaum. Human-level concept learning through probabilistic program induction. *Science*, 350(6266):1332–1338, 2015.
- [21] Alex Krizhevsky, Geoffrey Hinton, et al. Learning multiple layers of features from tiny images. 2009.
- [22] Grace XY Zheng, Jessica M Terry, Phillip Belgrader, Paul Ryvkin, Zachary W Bent, Ryan Wilson, Solongo B Ziraldo, Tobias D Wheeler, Geoff P McDermott, Junjie Zhu, et al. Massively parallel digital transcriptional profiling of single cells. *Nature communications*, 8(1):1–12, 2017.
- [23] Hodgkin’s Lymphoma, Dissociated Tumor: Targeted-Compare, Immunology Panel by Cell Ranger 4.0.0. *10x Genomics*, July 7th, 2020.
- [24] PBMCs from a Healthy Donor: Targeted, Immunology Panel by Cell Ranger 4.0.0. *10x Genomics*, July 7th, 2020.
- [25] John G Ratcliffe, S Axler, and KA Ribet. *Foundations of hyperbolic manifolds*, volume 149. Springer, 1994.
- [26] John M Lee. *Riemannian manifolds: an introduction to curvature*, volume 176. Springer Science & Business Media, 2006.
- [27] Jean H Gallier and Jocelyn Quaintance. *Differential Geometry and Lie Groups: A Computational Perspective*, volume 12. Springer Nature, 2020.
- [28] James W Cannon, William J Floyd, Richard Kenyon, Walter R Parry, et al. Hyperbolic geometry. *Flavors of geometry*, 31:59–115, 1997.
- [29] Vladimir Vapnik. *The nature of statistical learning theory*. Springer science & business media, 2013.
- [30] Loring W Tu. An introduction to manifolds. second, 2011.

- [31] Albert B Novikoff. On convergence proofs for perceptrons. Technical report, Stanford Research Institute, 1963.
- [32] Sanjoy Dasgupta, Adam Tauman Kalai, and Adam Tauman. Analysis of perceptron-based active learning. *Journal of Machine Learning Research*, 10(2), 2009.
- [33] Aravind Subramanian, Rajiv Narayan, Steven M Corsello, David D Peck, Ted E Natoli, Xiaodong Lu, Joshua Gould, John F Davis, Andrew A Tubelli, Jacob K Asiedu, et al. A next generation connectivity map: L1000 platform and the first 1,000,000 profiles. *Cell*, 171(6):1437–1452, 2017.

# SUPPLEMENTARY MATERIALS

## Contents

<b>1</b>	<b>Introduction</b>	<b>1</b>
<b>2</b>	<b>Linear Classifiers in Euclidean Space</b>	<b>2</b>
<b>3</b>	<b>Linear Classifiers in Space Forms</b>	<b>3</b>
3.1	Spherical Spaces . . . . .	4
3.2	Hyperbolic Spaces . . . . .	5
<b>4</b>	<b>Linear Classifiers in Product Space Forms</b>	<b>6</b>
4.1	A Product Space Form Perceptron . . . . .	7
4.1.1	Related Works and the Hyperbolic Perceptron . . . . .	8
4.2	A Product Space Form SVM . . . . .	8
<b>5</b>	<b>Numerical Experiments: Real-World Datasets</b>	<b>9</b>
<b>6</b>	<b>Proof of Proposition 1</b>	<b>14</b>
<b>7</b>	<b>Proof of Proposition 2</b>	<b>15</b>
<b>8</b>	<b>Proof of Theorem 1</b>	<b>16</b>
<b>9</b>	<b>Proof of Proposition 3</b>	<b>18</b>
<b>10</b>	<b>Proof of Theorem 2</b>	<b>18</b>
<b>11</b>	<b>Proof of Theorem 3</b>	<b>20</b>
11.1	Discussion . . . . .	21
<b>12</b>	<b>Proof of Proposition 4</b>	<b>21</b>
<b>13</b>	<b>Experiments</b>	<b>23</b>
13.1	Datasets . . . . .	23
13.2	Convergence Analysis of Hyperbolic Perceptron . . . . .	23
13.3	Synthetic Data . . . . .	24
13.4	Additional Real-World Datasets . . . . .	24
13.5	Supplementary Details for CIFAR-100 and scRNAseq Experiments . . . . .	25

Space forms are Riemannian manifolds of dimension  $d \geq 2$  that are isomorphic to spherical, Euclidean or hyperbolic spaces [26]. A  $d$ -dimensional spherical space with curvature  $C > 0$  is a collection of points  $\mathbb{S}^d = \{x \in \mathbb{R}^{d+1} : \langle x, x \rangle = C^{-1}\}$ , where  $\langle \cdot, \cdot \rangle$  is defined in the main text. Similarly, a  $d$ -dimensional hyperbolic space (i.e., the 'Loid model) with curvature  $C < 0$  is a collection of points of the form  $\mathbb{H}^d = \{x \in \mathbb{R}^{d+1} : [x, x] = C^{-1}\}$ , where  $[\cdot, \cdot]$  is defined in the main text. In Table 3, we list the Riemannian metric, exponential and logarithmic maps for each of these spaces. In sections B and C, we provide the proofs of Propositions 1 and 2 for space forms with arbitrary curvatures.

## 6 Proof of Proposition 1

Let  $p \in \mathbb{S}^d$  and  $w \in T_p \mathbb{S}^d = p^\perp$  such that  $\langle w, w \rangle = C$ . The separation surface  $H_{p,w}$  is defined as

$$\begin{aligned} H_{p,w} &= \{x \in \mathbb{S}^d : g_p(\log_p(x), w) = 0\} \\ &= \{x \in \mathbb{S}^d : \langle x, w \rangle = 0\}. \end{aligned}$$

We can compute the distance between  $x \in \mathbb{S}^d$  and  $H_{p,w}$  as

$$d(x, H_{p,w}) = \min_{y \in H_{p,w}} \frac{1}{\sqrt{C}} \operatorname{acos}(C y^\top x).$$

The projection of a point onto  $H_{p,w}$  can be computed by solving the following constrained optimization problem

$$\max_{y \in \mathbb{R}^{d+1}} x^\top y \quad \text{such that} \quad w^\top y = 0, \langle y, y \rangle = C^{-1}.$$

From the first order optimality condition for the Lagrangian, the projected point takes the form  $\mathcal{P}(x) = \alpha x + \beta w$ , where  $\alpha, \beta \in \mathbb{R}$ . Now, we impose the following subspace constraint,

$$\begin{aligned} w^\top \mathcal{P}(x) &= w^\top (\alpha x + \beta w) \\ &= \alpha w^\top x + \beta w^\top w \\ &= \alpha w^\top x + \beta C \\ &= 0, \end{aligned}$$

which gives  $\beta = -\alpha C^{-1} x^\top w$ . Subsequently, we have  $\mathcal{P}(x) = \alpha(x - C^{-1} x^\top w w)$ . On the other hand, from the norm constraint, we have

$$\begin{aligned} \|\mathcal{P}(x)\|^2 &= \alpha^2 (C^{-1} + C^{-1} (x^\top w)^2 - 2C^{-1} (x^\top w)^2) \\ &= \alpha^2 C^{-1} (1 - (x^\top w)^2) \\ &= C^{-1}, \end{aligned}$$

which gives  $\alpha = (1 - (x^\top w)^2)^{-\frac{1}{2}}$ . Then,

$$\mathcal{P}(x) = \sqrt{\frac{1}{1 - (x^\top w)^2}} \left( x - \frac{x^\top w}{w^\top w} w \right) = \sqrt{\frac{1}{1 - (x^\top w)^2}} P_w^\perp x = \frac{C^{-\frac{1}{2}}}{\|P_w^\perp x\|_2} P_w^\perp x, \quad (12)$$

where  $P_w^\perp x = x - \frac{1}{\langle w, w \rangle} \langle x, w \rangle w$ .

Table 3: Summary of relevant operators in Euclidean, spherical, and hyperbolic ('Loid model) spaces with arbitrary curvatures.

$\mathcal{M}$	$T_p \mathcal{M}$	$\mathcal{M} g_p(u, v)$	$\log_p(x) : \theta = \sqrt{ C } d(x, p)$	$\exp_p(v)$	$d(x, p)$
$\mathbb{R}^d$	$\mathbb{R}^d$	$\langle u, v \rangle$	$x - p$	$p + v$	$\ x - p\ _2$
$\mathbb{S}^d$	$p^\perp$	$\langle u, v \rangle$	$\frac{\theta}{\sin(\theta)} (x - p \cos \theta)$	$\cos(\sqrt{C} \ v\ ) p + \sin(\sqrt{C} \ v\ ) \frac{v}{\sqrt{C} \ v\ }$	$\frac{1}{\sqrt{C}} \operatorname{acos}(C \langle x, p \rangle)$
$\mathbb{L}^d$	$p^\perp$	$[u, v]$	$\frac{\theta}{\sinh(\theta)} (x - p \cosh \theta)$	$\cosh(\sqrt{-C} \ v\ ) p + \sinh(\sqrt{-C} \ v\ ) \frac{v}{\sqrt{-C} \ v\ }$	$\frac{1}{\sqrt{-C}} \operatorname{acosh}(C [x, p])$

Next, let us define  $\psi = \text{acos}(x^\top w)$ , where  $\psi \in [0, \pi]$ . Then, the minimum distance is given by

$$\begin{aligned}
d(x, \mathcal{P}(x)) &= \frac{1}{\sqrt{C}} \text{acos}(Cx^\top \mathcal{P}(x)) \\
&= \frac{1}{\sqrt{C}} \text{acos}\left(\sqrt{\frac{1}{1 - \cos^2 \psi}} (1 - \cos^2 \psi)\right) \\
&= \frac{1}{\sqrt{C}} \text{acos}(|\sin \psi|) \\
&\stackrel{\text{(a)}}{=} \frac{1}{\sqrt{C}} \text{asin}(|\cos \psi|) \\
&= \frac{1}{\sqrt{C}} \text{asin}|x^\top w|,
\end{aligned}$$

where (a) follows due to  $\text{acos}(|\sin(\psi)|) = \text{asin}(|\cos(\psi)|)$ , or

$$\begin{aligned}
\cos(\text{asin}(|\cos \psi|)) &= \cos\left(\text{asin}\left|\sin\left(\frac{\pi}{2} - \psi\right)\right|\right) \\
&= \cos\left|\text{asin}\left(\sin\left(\frac{\pi}{2} - \psi\right)\right)\right| \\
&= \cos\left|\frac{\pi}{2} - \psi\right| \\
&= |\sin \psi|,
\end{aligned}$$

for  $\psi \in [0, \pi]$ . Now, let  $x \in \mathbb{S}^d$ , and let  $\mathcal{P}(x)$  be as given in (12). We readily have  $\mathcal{P}(x) \perp w$ . Therefore,

$$\begin{aligned}
w^\top \log_{\mathcal{P}(x)}(x) &= \frac{\text{acos}(C\mathcal{P}(x)^\top x)}{\sin(\text{acos}(C\mathcal{P}(x)^\top x))} x^\top w \\
&\stackrel{\text{(a)}}{=} \frac{\text{acos}(C\mathcal{P}(x)^\top x)}{|x^\top w|} x^\top w \\
&= \text{asin}(|x^\top w|) \text{sgn}(x^\top w) \\
&= \text{asin}(x^\top w) = \text{sgn}(x^\top w) \sqrt{C} d(x, \mathcal{P}(x)),
\end{aligned}$$

where (a) follows from

$$\begin{aligned}
\sin(\text{acos}(C\mathcal{P}(x)^\top x)) &= \sin(\text{acos}(\sqrt{1 - (x^\top w)^2})) \\
&= \sin(\text{asin}(|x^\top w|)) \\
&= |x^\top w|.
\end{aligned}$$

This completes the proof.

## 7 Proof of Proposition 2

Let  $\mathbb{H}^d$  be the Poincaré model with curvature  $C < 0$  (usually set to  $C = -1$  for simplicity). The projection of  $x \in \mathbb{H}^d$  onto  $H_{p,w}$  is a point  $\mathcal{P}(x) \in H_{p,w}$  that has the smallest distance to  $x$ . In other words,  $\mathcal{P}(x)$  is the solution to the following constrained optimization problem

$$\max_y [y, x] \quad \text{such that } [y, y] = C^{-1}, [w, y] = 0,$$

where  $[w, w] = -C$ . The solution to this problem takes the form of  $\mathcal{P}(x) = \alpha x + \beta w$ , where  $\alpha, \beta \in \mathbb{R}$ . We can enforce the subspace condition as follows:

$$\begin{aligned}
[\mathcal{P}(x), w] &= \alpha[x, w] + \beta[w, w] \\
&= \alpha[x, w] + \beta(-C) \\
&= 0,
\end{aligned}$$



which gives  $\beta = \alpha C^{-1}[x, w]$ , or  $\mathcal{P}(x) = \alpha(x + C^{-1}[x, w]w)$ . On the other hand, we also have

$$\begin{aligned} [\mathcal{P}(x), \mathcal{P}(x)] &= \alpha^2(C^{-1} - C^{-1}[x, w]^2 + 2C^{-1}[x, w]^2) \\ &= \alpha^2 C^{-1}(1 + [x, w]^2) \\ &= C^{-1}. \end{aligned}$$

Then,

$$\mathcal{P}(x) = \sqrt{\frac{1}{1 + [x, w]^2}}(x + C^{-1}[x, w]w) = \frac{(-C)^{-\frac{1}{2}}}{\|P_w^\perp x\|} P_w^\perp x, \quad (13)$$

where  $P_w^\perp x = x - \frac{1}{[w, w]}[x, w]w$  and  $\|P_w^\perp x\| = \sqrt{-[P_w^\perp x, P_w^\perp x]}$ . The minimum distance can be computed as

$$\begin{aligned} d(x, \mathcal{P}(x)) &= \frac{1}{\sqrt{-C}} \operatorname{acosh}(C[\mathcal{P}(x), x]) \\ &= \frac{1}{\sqrt{-C}} \operatorname{acosh}\left(C \sqrt{\frac{1}{1 + [x, w]^2}} C^{-1}(1 + [x, w]^2)\right) \\ &= \frac{1}{\sqrt{-C}} \operatorname{acosh}(\sqrt{1 + [x, w]^2}). \end{aligned}$$

We can further simplify this expression to<sup>4</sup>:

$$d(x, \mathcal{P}(x)) = \frac{1}{\sqrt{-C}} \operatorname{asinh}([x, w]).$$

Now, let  $x \in \mathbb{L}^d$  and let  $\mathcal{P}(x)$  be given in (13). We can easily see that  $[\mathcal{P}(x), w] = 0$ . Therefore, we have

$$\begin{aligned} g_{\mathcal{P}(x)}(w, \log_{\mathcal{P}(x)}(x)) &= \frac{\operatorname{acosh}(C[\mathcal{P}(x), x])}{\sinh(\operatorname{acosh}(C[\mathcal{P}(x), x]))} [x, w] \\ &= \frac{\operatorname{asinh}([x, w])}{|[x, w]|} [x, w] \\ &= \operatorname{asinh}([x, w]) \operatorname{sgn}([x, w]) \\ &= \operatorname{asinh}([x, w]) = \operatorname{sgn}([x, w]) \sqrt{-C} d(x, \mathcal{P}(x)). \end{aligned}$$

This completes the proof.

## 8 Proof of Theorem 1

The Vapnik-Chervonenkis (VC) dimension [29] of a linear classifier is equal to the maximum size of a point set that a set of linear classifiers can *shatter*, i.e., completely partition into classes independent on how the point in the set are labelled. We establish the VC dimension for all three space forms  $\mathcal{M} = \mathbb{R}^d, \mathbb{S}^d$ , and  $\mathbb{L}^d$  (clearly, the VC dimension of Euclidean space forms is well-known, as described below).

The Vapnik-Chervonenkis (VC) dimension of affine classifiers in  $\mathbb{R}^d$  is  $d + 1$  (see the treatment of VC dimensions of Dudley classes described in [?]). Therefore, there exists a set of  $d + 1$  points that affine classifiers in  $\mathbb{R}^d$  can shatter. Note again the distinction between affine and linear classifiers in Euclidean spaces.

Next, let  $x_1, \dots, x_N \in \mathbb{S}^d$  be a set of point in spherical space  $\mathbb{S}^d$ , which can be shattered by linear classifiers. In other words, we have

$$y_n = \operatorname{sgn}(\operatorname{asin}(w_S^\top x_n)), \quad \forall n \in [N],$$

and for any set of binary labels  $(y_n)_{n \in [N]}$ . The linear classifiers in spherical space are a subset of linear classifiers in a  $(d + 1)$ -dimensional Euclidean space. Hence, their VC dimension must be less

<sup>4</sup>Since  $\cosh(x)^2 - \sinh(x)^2 = 1$ .

than or equal to  $d + 1$ . On the other hand, if we project a set of  $d + 1$  points in  $\mathbb{R}^{d+1}$  onto  $\mathbb{S}^d$ , that can be shattered by linear classifiers in Euclidean space (by a simple normalization). This way, we can find a set of (exactly)  $d + 1$  points that can be shattered by linear classifiers in  $\mathbb{S}^d$ . Hence, the VC dimension of linear classifiers in  $\mathbb{S}^d$  is exactly  $d + 1$ .

Next, let us turn our attention to  $d$ -dimensional hyperbolic spaces, namely the 'Loid model. Let  $\mathcal{X} = \{x_n\}_{n \in [d+1]}$  be a set of  $d + 1$  points in  $d$ -dimensional 'Loid model of hyperbolic space such that

$$x_n = \begin{bmatrix} \sqrt{1 + \|z_n\|^2} \\ z_n \end{bmatrix}$$

for  $z_n \in \mathbb{R}^d$  and all  $n \in [d + 1]$ . Furthermore, we assume that  $z_1 = 0$ , and  $z_n = e_{n-1}$  for  $n \in \{2, \dots, d + 1\}$ , where  $e_n$  is the  $n$ -th standard basis vector of  $\mathbb{R}^d$ .

We claim that this point set can be shattered by the set of linear classifiers in hyperbolic spaces, i.e.,

$$l_w^{\mathbb{H}}(x) = \text{sgn}(\text{asinh}([w, x])) \quad (14)$$

where  $w \in \{x \in \mathbb{R}^{d+1} : [x, x] > 0\}$ . Let  $(y_1, \dots, y_{d+1})$  be an arbitrary set of labels in  $\{-1, 1\}$ . Then, we define

$$\forall n \in \{2, \dots, d + 1\} : t_1 = y_1, t_n = ky_n \quad (15)$$

where  $k > \sqrt{2} + 1$ . Therefore, if we can show that there exists a  $w \in \{x \in \mathbb{R}^{d+1} : [x, x] > 0\}$  such that

$$\forall n \in [d + 1] : t_n = [w, x_n],$$

then we have  $y_n = l_w^{\mathbb{H}}(x_n)$  for all  $n \in [d + 1]$ . This is equivalent to showing that the following equation has a solution  $w \in \{x : [x, x] > 0\}$ ,

$$t = X^{\top} H w,$$

where  $t = (t_1, \dots, t_{d+1})$ , and

$$X^{\top} = \begin{bmatrix} \sqrt{1 + \|z_1\|^2} & z_1^{\top} \\ \sqrt{1 + \|z_2\|^2} & z_2^{\top} \\ \vdots & \vdots \\ \sqrt{1 + \|z_{d+1}\|^2} & z_{d+1}^{\top} \end{bmatrix} = \begin{bmatrix} 1 & 0^{\top} \\ \sqrt{2} & e_1^{\top} \\ \vdots & \vdots \\ \sqrt{2} & e_d^{\top} \end{bmatrix}.$$

The solution is  $w = H(X^{\top})^{-1}t$ , described below,

$$w = H \begin{bmatrix} 1 & 0^{\top} \\ -\sqrt{2} & e_1^{\top} \\ \vdots & \vdots \\ -\sqrt{2} & e_d^{\top} \end{bmatrix} t = \begin{bmatrix} -t_1 \\ -\sqrt{2}t_1 + t_2 \\ \vdots \\ -\sqrt{2}t_1 + t_{d+1} \end{bmatrix}.$$

As the final step, we show that  $w \in \{x : [x, x] > 0\}$ . To this end we observe that

$$\begin{aligned} [w, w] &= -t_1^2 + \sum_{n=2}^{d+1} (-\sqrt{2}t_1 + t_n)^2 \\ &\stackrel{(a)}{=} y_1^2 \left( -1 + \sum_{n=2}^{d+1} (-\sqrt{2} + k \frac{y_n}{y_1})^2 \right) \\ &\stackrel{(b)}{=} -1 + \sum_{n=2}^{d+1} (-\sqrt{2} + k \frac{y_n}{y_1})^2 \\ &\stackrel{(c)}{>} 0, \end{aligned}$$

where (a) is due to (15), (b) follows from  $y_n \in \{-1, 1\}$ , and (c) is obvious if  $k > \sqrt{2} + 1$ . Therefore, linear hyperbolic classifiers can generate any set of labels for the point set  $\{x_n\}_{n \in [d+1]}$ . Furthermore,

hyperbolic classifiers in (14) can be seen as linear classifiers in  $d + 1$  dimensional Euclidean space. Hence, the VC dimension of linear classifiers in hyperbolic space is exactly  $d + 1$ .

From Theorem 1 and the fundamental theorem of concept learning [? ], the function class  $\mathcal{L}$  is probably accurately correctly (PAC) learnable. More precisely, let  $\mathcal{P}$  be a family of probability distributions on  $\mathcal{M} \times \{-1, 1\}$ , and let  $\{(x_n, y_n)\}_{n \in [N]}$  be a set of i.i.d. samples from  $P \in \mathcal{P}$ . Then, we have

$$\inf_{l \in \mathcal{L}} P(\widehat{l}_N(X) \neq Y) \leq \inf_{l \in \mathcal{L}} P(l(X) \neq Y) + C \sqrt{\frac{d+1}{n}} + \sqrt{\frac{2 \log(\frac{1}{\delta})}{n}}$$

where  $\widehat{l}_N = \arg \min_{l \in \mathcal{L}} \frac{1}{N} \sum_{n \in [N]} 1(l(x_n) \neq y_n)$  is the empirical risk minimizer. Therefore, spherical, hyperbolic, and Euclidean linear classifiers have the same learning complexity.

### 9 Proof of Proposition 3

Let  $\mathcal{M} = \mathbb{E}^{d_{\mathbb{E}}} \times \mathbb{S}^{d_{\mathbb{S}}} \times \mathbb{H}^{d_{\mathbb{H}}}$  be a product space with the Riemannian metric  $g = \alpha_{\mathbb{E}} g^{\mathbb{E}} + \alpha_{\mathbb{S}} g^{\mathbb{S}} + \alpha_{\mathbb{H}} g^{\mathbb{H}}$ . Fact 1 gives us the logarithm map and tangent space at a point  $p = (p_{\mathbb{E}}, p_{\mathbb{S}}, p_{\mathbb{H}}) \in \mathcal{M}$ . A tangent vector  $w \in T_p \mathcal{M}$  can be expressed as  $w = (w_{\mathbb{E}}, w_{\mathbb{S}}, w_{\mathbb{H}})$  where  $w_{\mathbb{E}} \in T_{p_{\mathbb{E}}} \mathbb{E}^{d_{\mathbb{E}}}$ ,  $w_{\mathbb{S}} \in T_{p_{\mathbb{S}}} \mathbb{S}^{d_{\mathbb{S}}}$ , and  $w_{\mathbb{H}} \in T_{p_{\mathbb{H}}} \mathbb{H}^{d_{\mathbb{H}}}$ . From the point-line definition of linear classifiers (Definition 2), we have

$$\begin{aligned} l_{p,w}^{\mathcal{M}}(x) &= \text{sgn}(g_p(\log_p(x), w)) \\ &= \text{sgn}(\alpha_{\mathbb{E}} g_{p_{\mathbb{E}}}^{\mathbb{E}}(\log_{p_{\mathbb{E}}}(x_{\mathbb{E}}), w_{\mathbb{E}}) + \alpha_{\mathbb{S}} g_{p_{\mathbb{S}}}^{\mathbb{S}}(\log_{p_{\mathbb{S}}}(x_{\mathbb{S}}), w_{\mathbb{S}}) + \alpha_{\mathbb{H}} g_{p_{\mathbb{H}}}^{\mathbb{H}}(\log_{p_{\mathbb{H}}}(x_{\mathbb{H}}), w_{\mathbb{H}})). \end{aligned}$$

In Propositions 1 and 2, we derived specific spherical and hyperbolic base points to formalize distance-based classifiers. From these results, we may define a linear classifier in  $\mathcal{M}$  that is parameterized only with a tangent vector  $w$ , i.e.,

$$l_w^{\mathcal{M}}(x) = \text{sgn}((\alpha_{\mathbb{E}} w_{\mathbb{E}})^{\top} x_{\mathbb{E}} + b + \alpha_{\mathbb{S}} \text{asin}(w_{\mathbb{S}}^{\top} x_{\mathbb{S}}) + \alpha_{\mathbb{H}} \text{asinh}([w_{\mathbb{H}}, x_{\mathbb{H}}])) \quad (16)$$

where  $\|w_{\mathbb{E}}\| = 1$ ,  $\|w_{\mathbb{S}}\| = C_{\mathbb{S}}$ , and  $[w_{\mathbb{H}}, w_{\mathbb{H}}] = -C_{\mathbb{H}}$ . This completes the proof.

**Remark.** The linear classifier of (16) is not a distance-based classifier with respect to our choice of the Riemannian metric  $g$ . The distance between a point  $x$  and the classification boundary  $H_{p,w}$  can be computed as

$$\begin{aligned} d(x, H_{p,w}) &= \min_{y \in H_{p,w}} d(x, y) \\ &= \left( \alpha_{\mathbb{E}}^2 \|x_{\mathbb{E}} - y_{\mathbb{E}}^*\|^2 + \alpha_{\mathbb{S}}^2 \frac{1}{C_{\mathbb{S}}} \text{acos}^2(C_{\mathbb{S}} x_{\mathbb{S}}^{\top} y_{\mathbb{S}}^*) + \alpha_{\mathbb{H}}^2 \frac{1}{-C_{\mathbb{H}}} \text{acosh}^2(C_{\mathbb{H}} [x_{\mathbb{H}}, y_{\mathbb{H}}^*]) \right)^{1/2} \end{aligned}$$

where  $y^*$  is the projection of  $x$  onto the separation plane  $H_{p,w}$ . It is easy to verify that this distance is not related to the decision criteria, i.e.,  $(\alpha_{\mathbb{E}} w_{\mathbb{E}})^{\top} x_{\mathbb{E}} + b + \alpha_{\mathbb{S}} \text{asin}(w_{\mathbb{S}}^{\top} x_{\mathbb{S}}) + \alpha_{\mathbb{H}} \text{asinh}([w_{\mathbb{H}}, x_{\mathbb{H}}])$ , which only takes the weighted sum of (signed) distances between  $x_S$  and  $H_{p_S, w_S}$  for  $S \in \{\mathbb{E}, \mathbb{S}, \mathbb{H}\}$ .

### 10 Proof of Theorem 2

**Lemma 1.** Let  $K(x_1, x_2) = \text{asin}(x_1^{\top} x_2)$ , where  $x_1, x_2 \in B_{\circ} = \{x \in \mathbb{R}^d : \|x\|_2 \leq 1\}$ . Then, there exists a Hilbert space  $\mathcal{H}_{\circ}$ , and a mapping  $\phi_{\circ} : B_{\circ} \rightarrow \mathcal{H}_{\circ}$  such that

$$K(x_1, x_2) = \langle \phi_{\circ}(x_1), \phi_{\circ}(x_2) \rangle_{\mathcal{H}_{\circ}},$$

where  $\langle \cdot, \cdot \rangle_{\mathcal{H}_{\circ}}$  is the inner product on  $\mathcal{H}_{\circ}$ . Moreover, we can construct a space  $\mathcal{H}'_{\circ} \supset \mathcal{H}_{\circ}$  such that indefinite inner products of the form  $\langle \cdot, M_{\circ} \cdot \rangle_{\mathcal{H}'_{\circ}}$  are well-defined on  $\mathcal{H}'_{\circ}$ . The indefinite operator  $M_{\circ} : \mathcal{H}'_{\circ} \rightarrow \mathcal{H}'_{\circ}$  admits the following representation

$$K_H(x_1, x_2) = \text{asinh}(x_1^{\top} x_2) = \langle \phi_{\circ}(x_1), M_{\circ} \phi_{\circ}(x_2) \rangle_{\mathcal{H}'_{\circ}},$$

for all  $x_1, x_2$  in a compact subset of  $\mathbb{R}^d$ , and it satisfies  $M_{\circ}^{\top} M_{\circ} = \text{Id}$ , where  $\text{Id}$  denotes the identity operator.

*Proof.* The Taylor series expansion of  $\text{asin}$  can be used to establish that

$$\text{asin}(x_1^\top x_2) = \sum_{n=0}^{\infty} \frac{(2n)!}{2^{2n}(n!)^2(2n+1)} (x_1^\top x_2)^{2n+1}, \quad (17)$$

where  $|x_1^\top x_2| \leq 1$ . All the coefficients of this Taylor series are nonnegative. Hence, from Theorem 2.1 in [? ], this is a valid positive-definite kernel. Therefore, there is a Hilbert space  $\mathcal{H}_\circ$  endowed with an inner product  $\langle \cdot, \cdot \rangle_{\mathcal{H}_\circ}$  such that

$$\text{asin}(x_1^\top x_2) = \langle \phi_\circ(x_1), \phi_\circ(x_2) \rangle_{\mathcal{H}_\circ},$$

for  $x_1, x_2 \in B_\circ$  and vectors  $\phi_\circ(x_1)$  and  $\phi_\circ(x_2) \in \mathcal{H}_\circ$ .

On the other hand, we have

$$\text{asinh}(x_1^\top x_2) = \sum_{n=0}^{\infty} (-1)^n \frac{(2n)!}{2^{2n}(n!)^2(2n+1)} (x_1^\top x_2)^{2n+1},$$

where  $x_1, x_2 \in B \subseteq \mathbb{R}^d$  — a compact subset of  $\mathbb{R}^d$ . This Taylor series is the same as the one given in (17) except for the alternating signs of the coefficients. The analytical construction of the vector  $\phi_\circ(x)$  in [? ] gives a straightforward way to define an indefinite operator  $M_\circ : \mathcal{H}'_\circ \rightarrow \mathcal{H}'_\circ$  such that  $M_\circ^\top M_\circ = \text{Id}$ , and

$$\text{asinh}(x_1^\top x_2) = \langle \phi_\circ(x_1), M_\circ \phi_\circ(x_2) \rangle_{\mathcal{H}'_\circ}.$$

Note that  $M_\circ$  is a finite-dimensional diagonal matrix with elements  $\pm 1$  that represent the signs of the Taylor series coefficients.

The space  $\mathcal{H}'_\circ$  contains  $\mathcal{H}_\circ$  with the same definite inner product, i.e., if  $\phi_\circ(x), \phi_\circ(y) \in \mathcal{H}'_\circ \cap \mathcal{H}$ , then  $\langle \phi_\circ(x), \phi_\circ(y) \rangle_{\mathcal{H}_\circ} = \langle \phi_\circ(x), \phi_\circ(y) \rangle_{\mathcal{H}'_\circ}$ . However, a point  $\phi_\circ(x) \in \mathcal{H}'_\circ \setminus \mathcal{H}_\circ$  may have an unbounded norm, i.e.,  $\langle \phi_\circ(x), \phi_\circ(x) \rangle_{\mathcal{H}'_\circ} = \infty$ . Nevertheless, the indefinite inner products of the form  $\langle \phi_\circ(x), M_\circ \phi_\circ(x) \rangle_{\mathcal{H}'_\circ}$  are always well-defined so long as  $x \in B$ , a compact subset of  $\mathbb{R}^d$ . This is due to the fact that the convergence domain for the Taylor series of  $\text{asinh}(\cdot)$  is any compact subset of  $\mathbb{R}$ . Hence, we can simply define  $\mathcal{H}'_\circ = \{\phi_\circ(x) : x \in B \subset \mathbb{R}^d\}$ , where  $B$  is a compact subset of  $\mathbb{R}^d$ .  $\square$

Let  $\{x_1, \dots, x_N\}$  be a set of  $N$  points in the product space  $\mathcal{M}$ . For any point  $x = [x_\mathbb{E}, x_\mathbb{S}, x_\mathbb{H}] \in \mathcal{M}$ , we define

$$\phi(x) = \left(1, x_\mathbb{E}, \sqrt{\alpha_\mathbb{S}} \phi_\circ(\sqrt{C_\mathbb{S}} x_\mathbb{S}), \sqrt{\alpha_\mathbb{H}} \phi_\circ\left(H \frac{1}{R} x_\mathbb{H}\right)\right),$$

where  $\phi(x)$  is defined as in the proof of Lemma 1, and  $R$  is an upper bound for the norm of the hyperbolic component of  $x$ , i.e.,  $\|x_\mathbb{H}\|_2 \leq R$ . Note that in order to distinguish the curvatures of different space forms, we added appropriate subscripts.

The linear classifier in product space form can be written as

$$\begin{aligned} l_w^\mathcal{M}(x) &= \text{sgn}(w_\mathbb{E}^\top x_\mathbb{E} + b + \alpha_\mathbb{S} \text{asin}(w_\mathbb{S}^\top x_\mathbb{S}) + \alpha_\mathbb{H} \text{asinh}((Rw_\mathbb{H})^\top \frac{1}{R} H x_\mathbb{H})) \\ &= \text{sgn}(\langle \psi(w), M\phi(x) \rangle_{\mathcal{H}}), \end{aligned}$$

where  $\mathcal{H}$  is a simple product of  $\mathbb{R}^{d_\mathbb{E}+1}$ ,  $\mathcal{H}_\circ$  and  $\mathcal{H}'_\circ$  accompanied by their corresponding inner products,  $\psi(w) = (b, w_\mathbb{E}, \sqrt{\alpha_\mathbb{S}} \phi_\circ(\frac{1}{\sqrt{C_\mathbb{S}}} w_\mathbb{S}), \sqrt{\alpha_\mathbb{H}} \phi_\circ(Rw_\mathbb{H})) \in \mathcal{H}$ , and  $M = \text{diag}\{I, I, M_\circ\}$  is a product operator on  $\mathcal{H}$  such that

$$\langle \psi(w), M\phi(x) \rangle_{\mathcal{H}} = w_\mathbb{E}^\top x_\mathbb{E} + b + \alpha_\mathbb{S} \langle \phi_\circ(\frac{1}{\sqrt{C_\mathbb{S}}} w_\mathbb{S}), \phi_\circ(\sqrt{C_\mathbb{S}} x_\mathbb{S}) \rangle_{\mathcal{H}_\circ} + \alpha_\mathbb{H} \langle \phi_\circ(Rw_\mathbb{H}), M_\circ \phi_\circ(\frac{1}{R} H x_\mathbb{H}) \rangle_{\mathcal{H}'_\circ}.$$

From the problem assumptions, we assume the data points are linearly separable, i.e.,

$$\forall n \in [N] : y_n \langle w^*, M\phi(x_n) \rangle_{\mathcal{H}} \geq \varepsilon,$$

for a specific  $w^*$  in  $\mathcal{H}$ . Similar to the hyperbolic perceptron setting, we use the following update rule in RKHS

$$w^{k+1} = w^k + y_n M\phi(x_n) \text{ if } y_n \langle w^k, M\phi(x_n) \rangle_{\mathcal{H}} \leq 0.$$

If we initialize  $w^0 = 0 \in \mathcal{H}$ , we have

$$\begin{aligned}\langle w^*, w^{k+1} \rangle_{\mathcal{H}} &= \langle w^*, w^k \rangle_{\mathcal{H}} + \langle w^*, My_n \phi(x_n) \rangle_{\mathcal{H}} \\ &\geq \langle w^*, w^k \rangle_{\mathcal{H}} + \varepsilon \\ &\geq k\varepsilon.\end{aligned}$$

On the other hand, we can bound the norm as

$$\begin{aligned}\langle w^{k+1}, w^{k+1} \rangle_{\mathcal{H}} &= \langle w^k, w^k \rangle_{\mathcal{H}} + \langle y_n M \phi(x_n), y_n M \phi(x_n) \rangle_{\mathcal{H}} + 2 \langle w^k, y_n M \phi(x_n) \rangle_{\mathcal{H}} \\ &\leq \langle w^k, w^k \rangle_{\mathcal{H}} + \langle \phi(x_n), \phi(x_n) \rangle_{\mathcal{H}} \\ &\leq \langle w^k, w^k \rangle_{\mathcal{H}} + 1 + \|x_{\mathbb{E},n}\|_2^2 + \alpha_{\mathbb{S}} \langle \phi_{\circ}(\sqrt{C_{\mathbb{S}}} x_{\mathbb{S},n}), \phi_{\circ}(\sqrt{C_{\mathbb{S}}} x_{\mathbb{S},n}) \rangle_{\mathcal{H}_{\circ}} + \alpha_{\mathbb{H}} \langle \phi_{\circ}(\frac{1}{R} H x_{\mathbb{H},n}), \phi_{\circ}(\frac{1}{R} H x_{\mathbb{H},n}) \rangle_{\mathcal{H}'_{\circ}} \\ &\stackrel{(a)}{\leq} k(1 + R_{\mathbb{E}}^2 + (\alpha_{\mathbb{S}} + \alpha_{\mathbb{H}}) \frac{\pi}{2}),\end{aligned}$$

where  $R_{\mathbb{E}}$  is an upper bound for the norm of the Euclidean components of the vectors, and (a) is due to

$$\langle \phi_{\circ}(\sqrt{C_{\mathbb{S}}} x_{\mathbb{S},n}), \phi_{\circ}(\sqrt{C_{\mathbb{S}}} x_{\mathbb{S},n}) \rangle_{\mathcal{H}_{\circ}} = \text{asin}(C_{\mathbb{S}} x_{\mathbb{S},n}^{\top} x_{\mathbb{S},n}) = \frac{\pi}{2},$$

and

$$\langle \phi_{\circ}(\frac{1}{R} H x_{\mathbb{H},n}), \phi_{\circ}(\frac{1}{R} H x_{\mathbb{H},n}) \rangle_{\mathcal{H}'_{\circ}} = \text{asin}(\frac{1}{R^2} x_{\mathbb{H},n}^{\top} x_{\mathbb{H},n}) \leq \frac{\pi}{2}.$$

Hence,

$$\begin{aligned}\frac{(\langle w^{k+1}, w^* \rangle_{\mathcal{H}})^2}{\langle w^{k+1}, w^{k+1} \rangle_{\mathcal{H}} \langle w^*, w^* \rangle_{\mathcal{H}}} &\geq \frac{k^2 \varepsilon^2}{k B_T \langle w^*, w^* \rangle_{\mathcal{H}}} \\ &= k \frac{\varepsilon^2}{B_T \langle w^*, w^* \rangle_{\mathcal{H}}},\end{aligned}$$

where  $B_T = 1 + R_{\mathbb{E}}^2 + (\alpha_{\mathbb{S}} + \alpha_{\mathbb{H}}) \frac{\pi}{2}$ . Therefore, convergence is guaranteed in  $k \leq \frac{B_T \langle w^*, w^* \rangle_{\mathcal{H}}}{\varepsilon^2}$  steps. Finally, the upper bound for the  $\ell_2$  norm of  $w_{\mathbb{H}}$  guarantees the boundedness of  $\langle w^*, w^* \rangle_{\mathcal{H}}$ .

## 11 Proof of Theorem 3

Let  $w^0 = 0 \in \mathbb{R}^{d+1}$  and let  $w^k \in \mathbb{R}^{d+1}$  be the estimated normal vector at the  $k$ -th iteration of the perceptron algorithm (see Algorithm 3). If the point  $x_n \in \mathbb{L}^d$  ( $y_n [w^k, x_n] < 0$ ) is misclassified, the perceptron algorithm produces the  $(k+1)$ -th estimate of the normal vector according to

$$w^{k+1} = w^k + y_n H x_n.$$

Let  $w^*$  be the normal vector that classifies all the points with margin of at least  $\varepsilon$ , i.e.,  $y_n \text{asinh}([w^*, x_n]) \geq \varepsilon, \forall n \in [N]$ , and  $[w^*, w^*] = 1$ . Then, we have

$$\begin{aligned}(w^*)^{\top} w_{k+1} &= (w^*)^{\top} w^k + y_n [w^*, x_n] \\ &\geq (w^*)^{\top} w^k + \sinh(\varepsilon) \\ &\geq k \sinh(\varepsilon).\end{aligned}$$

In what follows, we provide an upper bound on  $\|w^{k+1}\|^5$ ,

$$\begin{aligned}\|w^{k+1}\|^2 &= \|w^k + y_n H x_n\|^2 \\ &= \|w^k\|^2 + \|x_n\|^2 + 2y_n [w^k, x_n] \\ &\stackrel{(a)}{\leq} \|w^k\|^2 + R^2 \\ &= kR^2,\end{aligned}$$

<sup>5</sup>Here, the norm is taken in the Euclidean sense, i.e.,  $\|w\| = \sqrt{w^{\top} w}$ .

where (a) is due to  $\|x_n\|^2 \leq R^2$  and  $y_n[w^k, x_n] \leq 0$ , due to the error in classifying the point  $x_n$ . Hence,

$$\|w^{k+1}\| \leq \sqrt{k}R \text{ and } (w^*)^\top w^{k+1} \geq k \sinh(\varepsilon). \quad (18)$$

To complete the proof, define  $\theta_k = \arccos\left(\frac{(w^k)^\top w^*}{\|w^k\| \|w^*\|}\right)$ . Then,

$$\begin{aligned} \frac{(w^{k+1})^\top w^*}{\|w^{k+1}\| \|w^*\|} &\stackrel{(a)}{\geq} \frac{k \sinh(\varepsilon)}{\sqrt{k}R \|w^*\|} \\ &= \sqrt{k} \frac{\sinh(\varepsilon)}{R \|w^*\|}, \end{aligned}$$

where (a) follows from (18). For  $k \geq \left(\frac{R \|w^*\|}{\sinh(\varepsilon)}\right)^2$ , we have  $w^{k+1} = \alpha_{k+1} w^*$  for a positive scalar  $\alpha_{k+1}$ . Hence,  $\frac{1}{\sqrt{[w^{k+1}, w^{k+1}]}} w^{k+1} = w^*$ .

## 11.1 Discussion

Linear classifiers in spherical spaces have been studied in a number of works [31, 32], while more recent work has focused on linear classifiers in the Poincaré model of hyperbolic spaces, in the context of hyperbolic neural networks [?]. A purely hyperbolic perceptron (in the same 'Loid model used in this work) was described in [17]. The proposed update rule reads as

$$u^k = w^k + y_n x_n \text{ if } -y_n[w^k, x_n] < 0 \quad (19)$$

$$w^{k+1} = u^k / \min\{1, \sqrt{[u^k, u^k]}\}, \quad (20)$$

where (20) is a ‘‘normalization step’’. Unfortunately, the above update rule does not allow the hyperbolic perceptron algorithm (Equations (19) and (20)) to converge, which is due to the choice of the update direction. The convergence issue is also illustrated by the following two examples.

Let  $x_1 = [\sqrt{2}, 1, 0]^\top \in \mathbb{L}^2$  with label  $y_1 = 1$ . We choose the initial vector in the update rule to be  $w^0 = \left[-\frac{\sqrt{2}+3}{4}, \frac{-1+3\sqrt{2}}{4}, 0\right]^\top$  (in contrast to  $w^0 = e_2$ , which was chosen in the proof [17]). This is a valid choice because  $[w^0, w^0] = \frac{1}{2} > 0$ . In the first iteration, we must hence update  $w^0$  since  $-y_1[w^0, x_1] = -\frac{1}{4} < 0$ . From (19), we have  $u^0 = w^0 + y_1 x_1 = \left[\frac{3\sqrt{2}+3}{4}, \frac{3+3\sqrt{2}}{4}, 0\right]^\top$ , and  $[u^0, u^0] = 0$ . This means that  $w^1 = \frac{1}{\sqrt{[u^0, u^0]}} u^0$  is clearly ill-defined.

As another example, let  $w^*$  be the optimal vector with which we can classify all data points with margin  $\varepsilon$ . If we simply choose  $w^0 = 0$ , then we can satisfy the required condition  $[w^0, w^*] \geq 0$  postulated for the hyperbolic perceptron. This leads to  $u^0 = x_1$ . Then, for any  $x_1 \in \mathbb{L}^2$ , we have  $[x_1, x_1] = -1$ , which leads to a normalization factor  $\sqrt{[u^0, u^0]}$  that is a complex number.

## 12 Proof of Proposition 4

Let  $\psi(w) = [b, w_{\mathbb{E}}, \sqrt{\alpha_{\mathbb{S}}}\phi_{\circ}\left(\frac{1}{\sqrt{C_{\mathbb{S}}}}w_{\mathbb{S}}\right), \sqrt{\alpha_{\mathbb{H}}}\phi_{\circ}(Rw_{\mathbb{H}})] = \sum_{n \in [N]} \beta_n M\phi(x_n)$ . We now consider the norm constraint for each component separately.

---

### Algorithm 3 Hyperbolic Perceptron

---

**Input:**  $\{x_n, y_n\}_{n=1}^N$ : a set of point-labels in  $\mathbb{H}^{d_{\mathbb{H}}} \times \{-1, 1\}$ .

**Initialization:**  $w^0 = 0 \in \mathbb{R}^{d_{\mathbb{H}}+1}$ ,  $k = 0$ ,  $n = 1$ .

**repeat**

**if**  $\text{sgn}([w^k, x_n]) \neq y_n$  **then**

$w^{k+1} = w^k + y_n H x_n$ ;

$k = k + 1$ ;

**end if**

$n = \text{mod}(n, N) + 1$ ;

**until** Convergence criteria is met.

---

The parameters for Euclidean component can be written as

$$b = \sum_{n \in [N]} \beta_n, \quad w_{\mathbb{E}} = \sum_{n \in [N]} \beta_n x_{\mathbb{E},n}$$

The distance-based Euclidean classifier asks for a vector such that  $\|w_{\mathbb{E}}^*\|_2 = \alpha_{\mathbb{E}}$ . We can impose this condition as a quadratic equality constraint on the vector  $\beta = (\beta_1, \dots, \beta_N)$  as follows

$$\|w_{\mathbb{E}}\|^2 = \beta^\top K_{\mathbb{E}} \beta = \alpha_{\mathbb{E}}^2,$$

where  $K_{\mathbb{E}} = (x_{\mathbb{E},i}^\top x_{\mathbb{E},j})_{i,j \in [N]}$ . The parameter of the spherical component can be written as

$$\phi_{\circ}\left(\frac{1}{\sqrt{C_{\mathbb{S}}}} w_{\mathbb{S}}\right) = \sum_{n \in [N]} \beta_n \phi_{\circ}(\sqrt{C_{\mathbb{S}}} x_{\mathbb{S},n})$$

A distance-based spherical classifier requires  $w_{\mathbb{S}} : \|w_{\mathbb{S}}\|_2 = \sqrt{C_{\mathbb{S}}}$ , i.e.,  $\phi_{\circ}\left(\frac{1}{\sqrt{C_{\mathbb{S}}}} w_{\mathbb{S}}\right)^\top \phi_{\circ}\left(\frac{1}{\sqrt{C_{\mathbb{S}}}} w_{\mathbb{S}}\right) = \text{asin}(1)$ . This is imposed by the following quadratic constraint

$$\left\| \phi_{\circ}\left(\frac{1}{\sqrt{C_{\mathbb{S}}}} w_{\mathbb{S}}\right) \right\|^2 = \beta^\top K_{\mathbb{S}} \beta = \frac{\pi}{2},$$

where  $K_{\mathbb{S}} = (\text{asin}(C_{\mathbb{S}} x_{\mathbb{S},i}^\top x_{\mathbb{S},j}))_{i,j \in [N]}$ . Finally, we can write the hyperbolic component as follows

$$\phi_{\circ}(Rw_{\mathbb{H}}) = \sum_{n \in [N]} \beta_n M_{\circ} \phi_{\circ}\left(\frac{1}{R} Hx_{\mathbb{H},n}\right).$$

The distance-based hyperbolic classifier  $w_{\mathbb{H}}$  must satisfy the norm constraint of  $[Rw_{\mathbb{H}}, Rw_{\mathbb{H}}] = -R^2 C_{\mathbb{H}}$ . Consequently, we must have

$$\phi_{\circ}(Rw_{\mathbb{H}})^\top M_{\circ} \phi_{\circ}(RHw_{\mathbb{H}}) = \text{asinh}(-R^2 C_{\mathbb{H}}).$$

**Lemma 2.**  $\phi_{\circ}(RHw_{\mathbb{H}}) = \sum_{i \in [N]} \beta_n M_{\circ} \phi_{\circ}\left(\frac{1}{R} x_{\mathbb{H},n}\right)$ .

*Proof.*

$$\begin{aligned} \text{asinh}(x_{\mathbb{H}}^\top w_{\mathbb{H}}) &= \phi_{\circ}\left(\frac{1}{R} x_{\mathbb{H}}\right)^\top M_{\circ} \phi_{\circ}(Rw_{\mathbb{H}}) \\ &\stackrel{(a)}{=} \sum_{n \in [N]} \beta_n \text{asin}\left(\frac{1}{R^2} [x_{\mathbb{H}}, x_{\mathbb{H},n}]\right) \\ &= \sum_{n \in [N]} \beta_n \phi_{\circ}\left(\frac{1}{R} Hx_{\mathbb{H}}\right)^\top M_{\circ} M_{\circ} \phi_{\circ}\left(\frac{1}{R} x_{\mathbb{H},n}\right) \\ &= \phi_{\circ}\left(\frac{1}{R} Hx_{\mathbb{H}}\right)^\top M_{\circ} \sum_{n \in [N]} \beta_n M_{\circ} \phi_{\circ}\left(\frac{1}{R} x_{\mathbb{H},n}\right) \end{aligned}$$

where (a) is due to  $\phi_{\circ}(Rw_{\mathbb{H}}) = \sum_{n \in [N]} \beta_n M_{\circ} \phi_{\circ}\left(\frac{1}{R} Hx_{\mathbb{H},n}\right)$ . From  $\text{asinh}(x_{\mathbb{H}}^\top w_{\mathbb{H}}) = \phi_{\circ}\left(\frac{1}{R} Hx_{\mathbb{H}}\right)^\top M_{\circ} \phi_{\circ}(RHw_{\mathbb{H}})$ , we have  $\phi_{\circ}(RHw_{\mathbb{H}}) = \sum_{n \in [N]} \beta_n M_{\circ} \phi_{\circ}\left(\frac{1}{R} x_{\mathbb{H},n}\right)$ .  $\square$

From the lemma, we have

$$\begin{aligned} \text{asinh}([Rw_{\mathbb{H}}, Rw_{\mathbb{H}}]) &= \phi_{\circ}(Rw_{\mathbb{H}})^\top M_{\circ} \phi_{\circ}(RHw_{\mathbb{H}}) \\ &= \sum_{i,j} \beta_i \beta_j \text{asinh}\left(\frac{1}{R^2} [x_{\mathbb{H},i}, x_{\mathbb{H},j}]\right) \\ &= \text{asinh}(-R^2 C_{\mathbb{H}}). \end{aligned}$$

The kernel matrix  $K_{\mathbb{H}} = (\text{asinh}\left(\frac{1}{R^2} [x_{\mathbb{H},i}, x_{\mathbb{H},j}]\right))_{i,j \in [N]}$  is an indefinite matrix. Therefore, we have the following non-convex second-order equality constraint

$$\phi_{\circ}^\top(Rw_{\mathbb{H}}) M_{\circ} \phi_{\circ}(RHw_{\mathbb{H}}) = \beta^\top K_{\mathbb{H}} \beta = \text{asinh}(-R^2 C_{\mathbb{H}}).$$



## 13 Experiments

We present additional experimental results that are not covered in the main text. All experiments were conducted on a Linux machine with 48 cores, 376GB of system memory.

### 13.1 Datasets

MNIST<sup>6</sup> [19], Omniglot<sup>7</sup> [20], CIFAR-100<sup>8</sup> [21], and single-cell expressions [22–24]<sup>9</sup> are publicly available datasets. Specific details of the three single-cell expressions data sets are as follows:

1. *Lymphoma patient.* Human dissociated lymph node tumor cells of a 19-year-old male Hodgkin’s Lymphoma patient were obtained by 10x Genomics from Discovery Life Sciences. Whole transcriptome libraries were generated with Chromium Next GEM Single Cell 3’ Reagent Kits v3.1 (Dual Index) User Guide (CG000315) and sequenced on an Illumina NovaSeq 6000. The targeted libraries were generated using the Targeted Gene Expression Reagent Kits User Guide (CG000293) and Human Immunology Panel reagent (PN-1000246) and sequenced on an Illumina NovaSeq 6000.
2. *Lymphoma-healthy donor.* Human peripheral blood mononuclear cells (PBMCs) of a healthy female donor aged 25 were obtained by 10x Genomics from AllCells. Whole transcriptome libraries were generated with Chromium Next GEM Single Cell 3’ Reagent Kits v3.1 (Dual Index) User Guide (CG000315) and sequenced on an Illumina NovaSeq 6000. The aforementioned two datasets have 13410 samples (combined) and each for a class (binary classification). The dimension of each cell expression vector is 1020 (both datasets).
3. *Blood cells landmark.* We use the dataset originally from this paper and extract the gene expression data for (1) B cells, (2) Cd14 monocytes, (3) Cd34 monocytes, (4) Cd4 t helper cells, (5) Cd56 natural killer cells, (6) Cytotoxic T cells, (7) Memory T cells, (8) Naive cytotoxic cells, (9) Native T cells, and (10) Regulatory T cells. This dataset has 94655 samples from the total 10 classes. The dimension of each cell expression vector is 965.

### 13.2 Convergence Analysis of Hyperbolic Perceptron

As pointed out in Section 11.1, the hyperbolic perceptron described in [17] does not converge, which can be shown both through counterexamples and simulation studies. We report the following experimental results to validate this point and in particular, demonstrate that a convergence rate of  $O\left(\frac{1}{\sinh(\varepsilon)}\right)$  is not possible.

First, we randomly generate a valid  $w^*$  such that  $[w^*, w^*] = 1$ . Then, we generate a random set of  $N = 5,000$  points  $\{x_i\}_{i=1}^N$  in  $\mathbb{L}^2$ . For margin values  $\varepsilon \in [0.1, 1]$ , we remove points that violate the required distance to the classifier (parameterized with  $w^*$ ), i.e., we decimate the points so that the condition  $\forall n : |[w^*, x_n]| \geq \sinh(\varepsilon)$  is satisfied. Then, we assign binary labels to each data point according to the optimal classifier, so that  $y_n = \text{sgn}(\text{asinh}([w^*, x_n]))$ . We repeat this process for 100 different values of  $\varepsilon$ .

In the first experiment, we compare our proposed hyperbolic perceptron Algorithm 3 and the Algorithm 1 in [17] by running the methods until the number of updates achieved a predetermined upper bound (stated in Theorem 3) or until the classifier correctly classified all the data points. In Figure 4 (a), we report the classification accuracy of each method on the training data. Note that our theoretically established convergence rate  $O\left(\frac{1}{\sinh^2(\varepsilon)}\right)$  is larger than  $O\left(\frac{1}{\sinh(\varepsilon)}\right)$ , the rate derived in Theorem 3.1 in [17]. So, for the second experiment, we repeated the same process but terminate both algorithms after  $O\left(\frac{1}{\sinh(\varepsilon)}\right)$  updates. The classification performance of the two algorithms under this setting is shown in Figure 4 (b). From these results, we can easily conclude that (1) our algorithm always converge within the theoretical upper bound provided in Theorem 3, and (2) both methods violate the theoretical convergence rate upper bound of [17].

<sup>6</sup><http://yann.lecun.com/exdb/mnist/>

<sup>7</sup><https://github.com/brendenlake/omniglot>

<sup>8</sup><https://www.cs.toronto.edu/~kriz/cifar.html>

<sup>9</sup>We used two data sets: Lymphoma patient vs. healthy donor, and blood cells landmark.

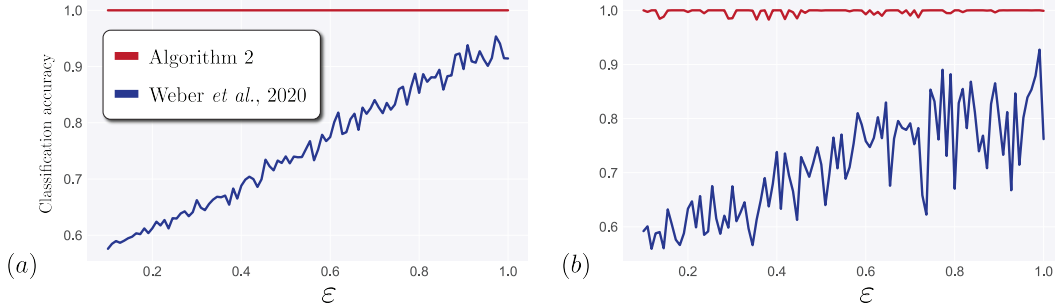


Figure 4: A comparison between the classification accuracy of our hyperbolic perceptron Algorithm 3 and the algorithm in [17] for different values of the margin  $\varepsilon$ . The classification accuracy is the average of five independent random trials. The stopping criterion is either a 100% classification accuracy or the theoretical upper bound in Theorem 3 (Figure (a)), and Theorem 3.1 in [17] (Figure (b)).

### 13.3 Synthetic Data

We illustrate the practical performance of our product space form perceptron Algorithm 1 on both synthetic and real-world datasets. In order to establish the benefits of product space form embeddings and learning, we compare our results with those obtained by using a Euclidean perceptron. As is a common approach for perceptron methods, we evaluate the classification accuracy on the training sets. To ensure a fair comparison, we restrict the latent dimension of the embeddings of both methods to be the same, meaning that data points lie in  $\mathbb{E}^{d_{\mathbb{E}}} \times \mathbb{S}^{d_{\mathbb{S}}} \times \mathbb{H}^{d_{\mathbb{H}}}$  for the product space form perceptron and in  $\mathbb{E}^{d_{\mathbb{E}}+d_{\mathbb{S}}+d_{\mathbb{H}}}$  for the Euclidean perceptron.

We generate binary-labeled synthetic data satisfying a  $\varepsilon$ -margin assumption as follows. First, we randomly and independently sample  $N$  points from a Gaussian distribution in each of the three spaces  $\mathbb{E}^2, \mathbb{E}^3, \mathbb{E}^3$ ; subsequently, we project the points in  $\mathbb{E}^3$  and  $\mathbb{E}^3$  onto  $\mathbb{S}_1^2$  and  $\mathbb{H}_{-1}^2$ , respectively. Then, we concatenate the coordinates from the three space form components to obtain the product space form embeddings. Finally, we randomly generate the optimal decision hyperplane  $w^* = (w_{\mathbb{E}}^*, 0, w_{\mathbb{S}}^*, w_{\mathbb{H}}^*)$  under the constraints stated in Theorem 1 and assign binary labels to data points. To ensure that the  $\varepsilon$ -margin assumption is satisfied, we translate points that violate this assumption.

We use the same data for both the Euclidean and product space form perceptron to demonstrate the efficiency and performance gains of the former method. This is because our method respects the geometry of data, whereas the purely Euclidean setting assumes input data lies in  $\mathbb{E}^8$ . In Figure 5, we show four different typical experimental convergence plots for  $N = 300$  points with the same optimal decision hyperplane  $w^*$ , but with different separation margins, i.e.,  $\varepsilon$ . We observe that the number of updates made by the product space form perceptron is always smaller than the theoretical upper bound provided in Theorem 1. When the margin is small, the data is not linearly separable in Euclidean space and the Euclidean perceptron does not converge to a 100% accurate solution. As  $\varepsilon$  increases, the data becomes easy to classify for both algorithms, and the number of updates made by the Euclidean perceptron decreases. The performance guarantees of the proposed methods is *independent* of the size of datasets.

We now fix the optimal decision hyperplane  $w^*$ . In Figure 6, we show nine more experiments with different combinations of  $(N, \varepsilon)$ . We observe that the number of updates made by the product space form perceptron is always smaller than the theoretical upper bound described in Theorem 2. And, in most cases, the product space form perceptron requires a smaller number of updates to converge than the Euclidean perceptron due to the fact that it accounts for the geometry of the data.

### 13.4 Additional Real-World Datasets

Following the procedure introduced in the work on mixed-curvature VAEs [18] (under license ASL 2.0),<sup>10</sup> we embed the MNIST and Omniglot data sets into the product space  $\mathbb{E}^2 \times \mathbb{S}^2 \times \mathbb{L}^2$ . For

<sup>10</sup>Code can be found at <https://github.com/oskopek/mvae>.

MNIST dataset, the curvatures of the hyperbolic and spherical spaces are  $-0.129869$  and  $0.286002$ . For Omniglot dataset, these curvatures are  $-0.173390$  and  $0.214189$ . Our experiments reveal that although the difference in the log-likelihood metric used to measure the quality of the mixed-curvature VAE and the Euclidean embedding is very small (see the results reported in [18] and reproduced in Table 4). The datasets of interest include MNIST, containing images of handwritten digits [19], and Omniglot, containing handwritten characters from a variety of world alphabets [20]. As suggested in [?] and [?], we downsample each image (in both datasets) to  $28 \times 28$  pixels and preprocess it by a dynamic-binarization procedure. Then we use the mixed-curvature VAE from [18] with default parameters to obtain a mixed-curvature embedding in  $\mathbb{E}^2 \times \mathbb{S}^2 \times \mathbb{H}^2$  and Euclidean embedding in  $\mathbb{E}^6$ . In these datasets, embedded points from different classes are not guaranteed to be linearly separable. Hence, we set both perceptron algorithms to terminate after going through a fixed maximum number of passes. Subsequently, we compute the Macro F1 scores to determine the quality of the learned linear classifiers. For simplicity, we only report ternary classification results for both datasets, including 500 points from three randomly chosen classes from MNIST and 20 points from three randomly chosen classes from Omniglot.

These datasets containing more than two classes. To enable  $K$ -class perceptron classification, we use  $K$  binary classifiers — represented by parameters  $w^{(i)}, i = 1, \dots, K$  — that are independently trained on the same training set to separate each single class from the remaining classes. For each classifier, we transform the resulting prediction scores into probabilities via the Platt scaling technique [?]. The predicted labels are decided by maximum a posteriori criteria, using the probability of each class.

We show the performance of the ternary classifiers in Figure 7. This is obtained by randomly selecting 100 sets of three classes; each point in the figure corresponds to one such combination, and its coordinate value equals the averaged Macro F1 score of three independent runs. Red-colored points indicate better performance of the product space form perceptron, while blue-colored points indicate better performance of the Euclidean perceptron. We observe that the product space form perceptron classifies almost twice as many sets with higher accuracy compared to its Euclidean counterpart. The performance gain of the product space form perceptron compared to the Euclidean perceptron (average gain in Marco F1 scores) is 0.2% for MNIST and 1.27% for Omniglot. This shows that the proposed product space form perceptron algorithm better use the features from a product space form to perform the learning task.

### 13.5 Supplementary Details for CIFAR-100 and scRNAseq Experiments

We embed each dataset using mixed-curvature VAEs. Specifically, we are using architecture MLP (ff) for scRNA sequencing dataset (epochs=300, likelihood=500) and convolution block (conv) for CIFAR-100 (epochs=200, likelihood=100).

*Perceptron:* For datasets with multiple classes, we perform binary classification by randomly choosing samples from two classes and report the confidence interval for classification results (over 10 repeated trials). For CIFAR-100 dataset, we only choose 100 class pairs whereas for the blood cell dataset with landmark gene, we test all  $\binom{10}{2} = 45$  pairs. Note that Lymphoma and Lymphoma-healthy donor labels are used for one binary classification problem.

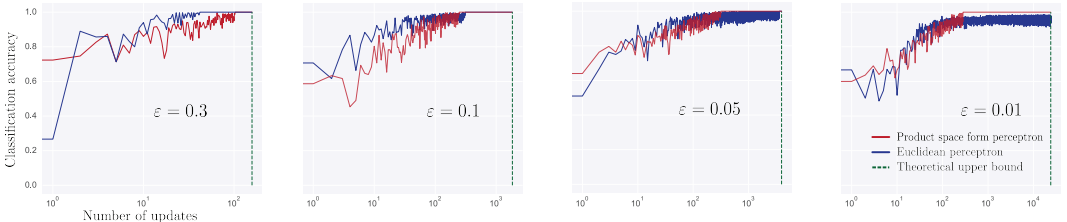


Figure 5: Classification accuracy after each update of the Euclidean and product space form perceptron algorithms for  $N = 300$  and different values of  $\epsilon$ .

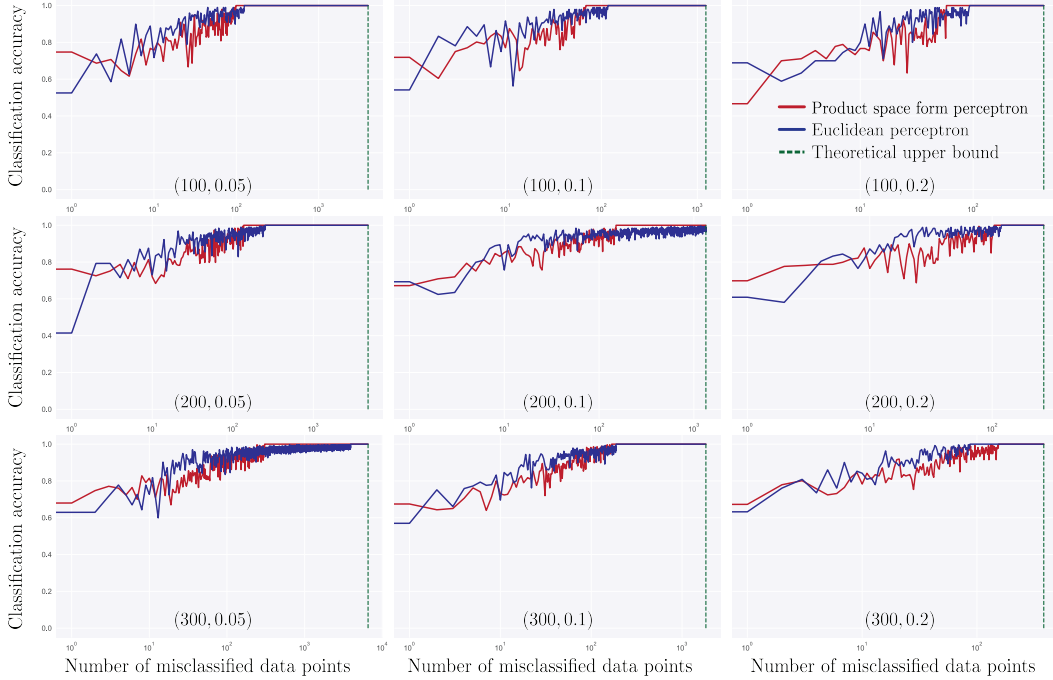


Figure 6: Classification accuracy after each update of the Euclidean and product space form perceptron algorithms for nine different combinations of  $(N, \varepsilon)$ .

*SVM*: For simplicity, we let  $\alpha_{\mathbb{E}} = \alpha_{\mathbb{S}} = \alpha_{\mathbb{H}} = 1$  in our implementation. Hyperbolic SVM is adopted from previous work [16].<sup>11</sup> In Table 5, we summarize the extended the classification results on CIFAR-100 dataset (over 10 repeated trials) which we covered in the main text.

Table 4: Estimated marginal log-likelihood after embedding the data into lower-dimensional spaces.

	MNIST	Omniglot
$\mathbb{E}^6$	$-96.88 \pm 0.16$	$-136.05 \pm 0.29$
$\mathbb{E}^2 \times \mathbb{S}_{\mathbb{C}_{\mathbb{S}}}^2 \times \mathbb{H}_{\mathbb{C}_{\mathbb{H}}}^2$	$-96.71 \pm 0.19$	$-135.93 \pm 0.48$

<sup>11</sup>The code can be found in <https://github.com/hhcho/hyplinear>

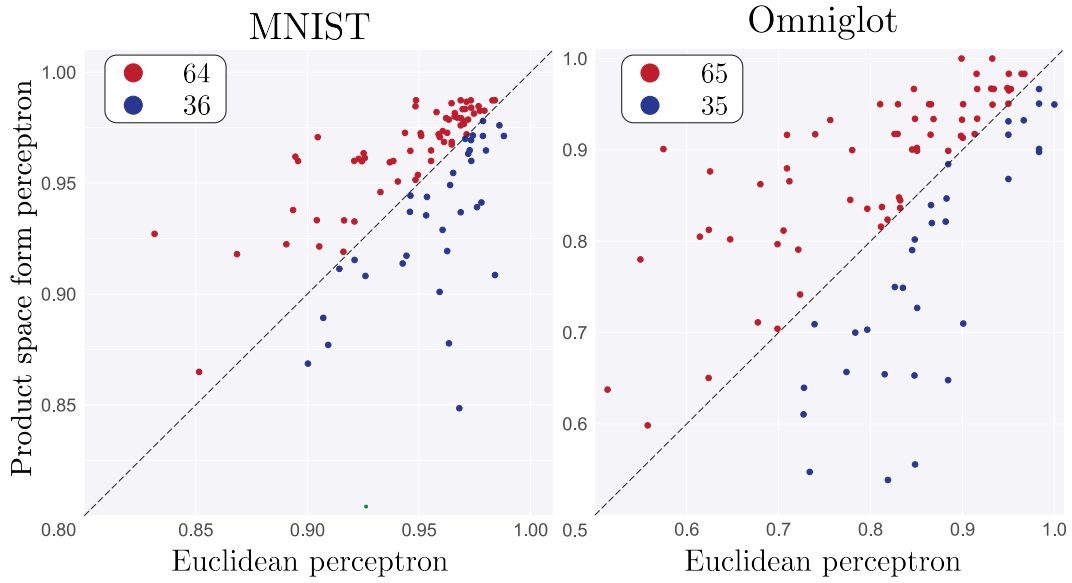


Figure 7: Comparison of Macro F1 scores of the Euclidean and product space form perceptron on MNIST and Omniglot.

Table 5: Classification mean accuracy (%)  $\pm$  95% confidence interval for perceptron (P) and SVM (S) algorithms in a product space  $(d_E, d_H, d_S)$ . Datasets are CIFAR-100 (CFR).

$(d_E, d_H, d_S)$	(2, 2, 2)	(6, 0, 0)	(0, 6, 0)	$(2, 2^2, 2)$	(2, 4, 2)	(8, 0, 0)	(0, 8, 0)
(P)-CFR	70.26 $\pm$ 1.34	68.58 $\pm$ 1.29	66.69 $\pm$ 0.95	<b>71.23 <math>\pm</math> 1.28</b>	69.93 $\pm$ 1.25	69.96 $\pm$ 1.29	69.90 $\pm$ 1.43
(S)-CFR	69.51 $\pm$ 0.66	<b>75.69 <math>\pm</math> 0.58</b>	70.91 $\pm$ 0.93	73.05 $\pm$ 0.62	62.02 $\pm$ 0.10	74.53 $\pm$ 0.56	70.65 $\pm$ 0.93